

ConfigX: Modular Configuration for Evolutionary Algorithms via Multitask Reinforcement Learning

Hongshu Guo^{1*}, Zeyuan Ma^{1*}, Jiacheng Chen¹, Yining Ma²,
Zhiguang Cao³, Xinglin Zhang¹, Yue-Jiao Gong^{1†}

¹South China University of Technology, ²Massachusetts Institute of Technology, ³Singapore Management University

Abstract

Recent advances in Meta-learning for Black-Box Optimization (MetaBBO) have shown the potential of using neural networks to dynamically configure evolutionary algorithms (EAs), enhancing their performance and adaptability across various BBO instances. However, they are often tailored to a specific EA, which limits their generalizability and necessitates retraining or redesigns for different EAs and optimization problems. To address this limitation, we introduce ConfigX, a new paradigm of the MetaBBO framework that is capable of learning a universal configuration agent (model) for boosting diverse EAs. To achieve so, our ConfigX first leverages a novel modularization system that enables the flexible combination of various optimization sub-modules to generate diverse EAs during training. Additionally, we propose a Transformer-based neural network to meta-learn a universal configuration policy through multitask reinforcement learning across a designed joint optimization task space. Extensive experiments verify that, our ConfigX, after large-scale pre-training, achieves robust zero-shot generalization to unseen tasks and outperforms state-of-the-art baselines. Moreover, ConfigX exhibits strong lifelong learning capabilities, allowing efficient adaptation to new tasks through fine-tuning. Our proposed ConfigX represents a significant step toward an automatic, all-purpose configuration agent for EAs.

1 Introduction

Over the decades, Evolutionary Algorithms (EAs) such as Genetic Algorithm (GA) (Holland 1992), Particle Swarm Optimization (PSO) (Kennedy and Eberhart 1995) and Differential Evolution (DE) (Storn and Price 1997) have been extensively researched to tackle challenging Black-Box Optimization (BBO) problems, where neither the mathematical formulation nor additional derivative information is accessible. On par with the development of EAs, one of the most crucial research avenues is the Automatic Configuration (AC) for EAs (Ansótegui, Sellmann, and Tierney 2009; Huang, Li, and Yao 2019). Generally speaking, AC for EAs aims at identifying the optimal configuration c^* from the configuration space \mathcal{C} of an evolutionary algorithm A , across a set of BBO problem instances \mathcal{I} :

$$c^* = \arg \max_{c \in \mathcal{C}} \mathbb{E}_{p \in \mathcal{I}} [Perf(A, c, p)] \quad (1)$$

*These authors contributed equally.

†Corresponding author.

where $Perf()$ denotes the performance of a configuration for the algorithm under a given problem instance.

Traditionally, the primary research focus in AC for EAs has centered on human-crafted AC mechanisms. These mechanisms, including algorithm/operator selection (Fialho 2010) and parameter control (Aleti and Moser 2016), have demonstrated strong performance on well-known BBO benchmarks (Hansen et al. 2010; Li et al. 2013; Li, Engelbrecht, and Epitropakis 2013), as well as in various eye-catching real-world scenarios such as Protein-Docking (Hwang et al. 2010), AutoML (Vanschoren et al. 2014), and Prompting Optimization of Large Language Models (Chen, Dohan, and So 2024). However, a major limitation of manual AC is its heavy reliance on deep expertise. To address a specific problem, one often needs to consult experts with the necessary experience to analyze the problem and then design appropriate AC mechanisms (as depicted in the top of Figure 1). This impedes the broader application of EAs in diverse scientific or industrial applications.

Recently, a novel paradigm called Meta-learning for Black-Box Optimization (MetaBBO) (Ma et al. 2023), has emerged in the learning-to-optimize community. MetaBBO aims to reduce the reliance on expert-level knowledge in designing more automated AC mechanisms. As shown in the middle of Figure 1, in MetaBBO, a neural network is meta-trained as a meta-level policy to maximize the expected performance (Eq. (1)) of a low-level algorithm by dictating suitable configuration for solving each problem instance. By leveraging the data-driven features of deep models and the generalization strengths of meta-learning (Finn, Abbeel, and Levine 2017) across a distribution of optimization problems, these MetaBBO methods (Chen et al. 2024; Li et al. 2024; Song et al. 2024) have shown superior adaptability compared to traditional human-crafted AC baselines.

Despite these advancements, there remains significant potential to further reduce the expertise burden. Current MetaBBO methods often need custom neural network designs, specific learning objectives, and frequent retraining or even complete redesigns to fit different backbone EAs, overlooking the shared aspects of AC across multiple EAs. This leads to the core research question of this paper: *Is it possible to develop a MetaBBO paradigm that can meta-learn an automatic, all-purpose configuration agent for diverse EAs?*

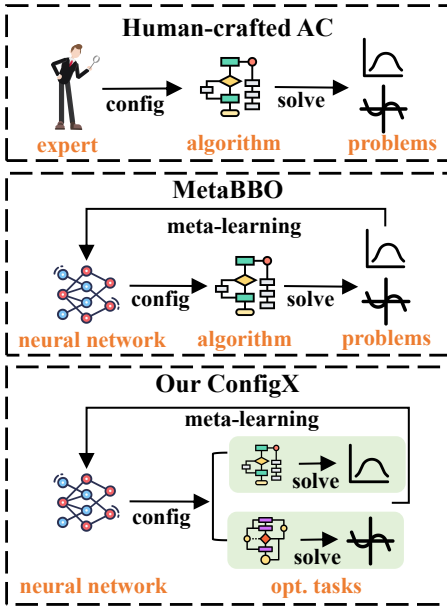


Figure 1: Conceptual overview of different AC paradigms.

We outline the detailed research objective below:

$$c_k^* = \arg \max_{c \in \mathcal{C}_k} \mathbb{E}_{p \in \mathcal{I}} [Perf(A_k, c, p)], k = 1, 2, \dots, K \quad (2)$$

where K is an exceedingly large number, potentially infinite. This objective is far more challenging since it can be regarded as the extension of Eq. (1). Concretely, it presents two key challenges: 1) **Constructing a comprehensive evolutionary algorithm space** is crucial for addressing Eq. (2), from which diverse EAs can be easily sampled for meta-training the MetaBBO; 2) **Ensuring the generalization capability** of the learned meta-level policy across not only optimization problems but also various EAs is imperative.

To address these challenges, we introduce ConfigX, a pioneering MetaBBO framework capable of modularly configuring diverse EAs with a single model across different optimization problems (as shown at the bottom of Figure 1).

Specifically, to address the first challenge, we present a novel modularization system for EAs, termed Modular-BBO in Section 3.1. It leverages hierarchical polymorphism to efficiently encapsulate and maintain various algorithmic sub-modules within the EAs, such as mutation or crossover operators. By flexibly combining these sub-modules, Modular-BBO can generate a vast array of distinct EA structures, hence spanning a comprehensive algorithm space \mathcal{A} . To address the second challenge, we combine the problem instance space \mathcal{I} and \mathcal{A} to form a joint optimization task space $\mathcal{T} : \mathcal{A} \times \mathcal{I}$. We then consider meta-learning a Transformer based meta-level policy over moderate optimization tasks sampled from the joint space \mathcal{T} to maximize the objective in Eq. (2), see Section 3.2 and 3.3. For each task $T = (A_m, I_n)$, the Transformer generates configurations by conditioning on a sequence of state tokens corresponding to the sub-modules in A_m . Through large-scale multitask reinforcement learning over the sampled tasks, it yields a univer-

sal meta-policy that exhibits robust generalization to unseen algorithm structures and problem instances.

We summarize our contributions in this paper in three folds:

- We introduce ConfigX, the first MetaBBO framework to learn a pre-trained universal AC agent via multitask reinforcement learning, enabling modular configuration of diverse EAs across various optimization problems.
- Technically, we present Modular-BBO as a novel system for EA modularization that simplifies the management of sub-modules and facilitates the sampling of diverse algorithm structures. We then propose a Transformer-based architecture to meta-learn a universal configuration policy over our defined joint optimization task space.
- Extensive benchmark results show that the configuration policy pre-trained by ConfigX not only achieves superior zero-shot performance against the state-of-the-art AC software SMAC3, but also exhibits favorable lifelong learning capability via efficient fine-tuning.

2 Related Works

2.1 Human-crafted AC

Human-crafted AC mechanisms enhance the optimization robustness of EAs through two main paradigms: Operator Selection (OS) and Parameter Control (PC). OS is geared towards selecting proper evolutionary operators (i.e., mutation in DE (Qin and Suganthan 2005)) for EAs to solve target optimization problems. To this end, such AC mechanism requires preparing a group of candidate operators with diverse searching behaviours. Besides, throughout the optimization progress, OS facilitates dynamic selection over the candidate operators, either by a roulette wheel upon the historical success rates (Lynn and Suganthan 2017) or random replacement upon the immediate performance improvement (Mallipeddi et al. 2011). PC, on the other hand, aims at configuring (hyper-) parameters for the operators in EAs, (e.g. the inertia weights in PSO (Amoshahy, Shamsi, and Sedaaghi 2016) and the scale factors in DE (Zhang and Sanderson 2009; Tanabe and Fukunaga 2013)), while embracing similar adaptive mechanisms as OS to achieve dynamic configuration. We note that OS and PC are complementary rather than conflicting. Recent outperforming EAs such as MadDE (Biswas et al. 2021), AMCDE (Ye et al. 2023) and SAHLPSO (Tao et al. 2021) integrate both to obtain maximal performance gain. However, the construction of the candidate operators pool, the parameter value range in PC, and the adaptive mechanism in both of them heavily rely on expertise. A more versatile and efficient alternative for human-crafted AC is Bayesian Optimization (BO) (Shahriari et al. 2015). By iteratively updating and sampling from a posterior distribution over the algorithm configuration space, a recent open-source BO software SMAC3 (Lindauer et al. 2022) achieves the state-of-the-art AC performance on many realistic scenarios.

2.2 MetaBBO

To relieve the expertise dependency of human-crafted AC, recent MetaBBO works introduce neural network-based

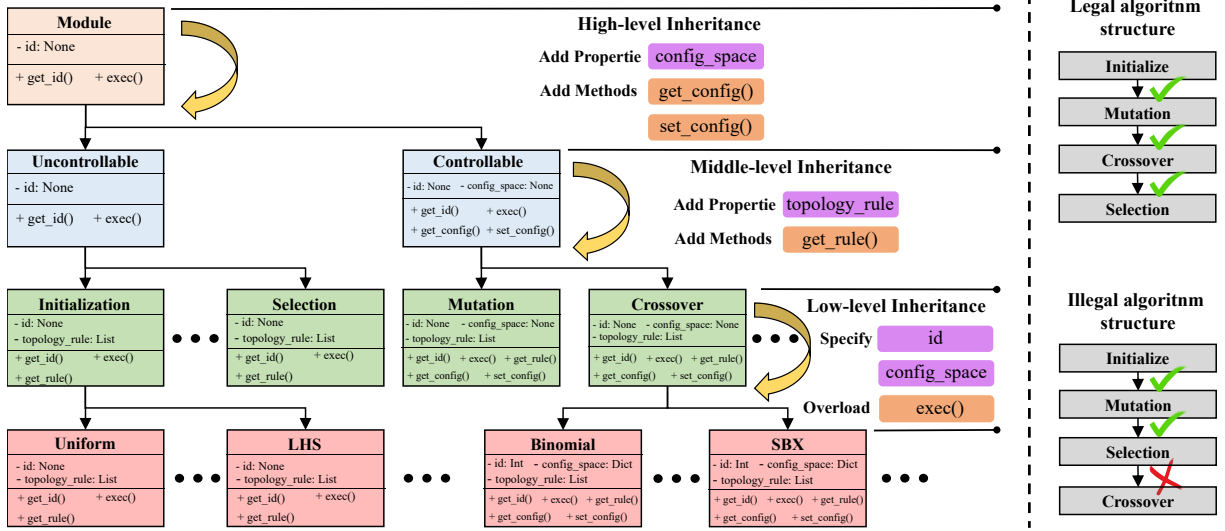


Figure 2: **Left:** The hierarchical polymorphism in Modular-BBO. **Right:** Legal/Illegal algorithm examples in Modular-BBO.

Algorithm 1: Algorithm Structure Generation.

Input: All accessible modules \mathbb{M} , all Initialization modules \mathbb{M}_{init}

Output: A legal algorithm structure A .

- 1: Create an empty structure $A = \emptyset$, set index $j = 0$
- 2: Randomly select an Initialization module from \mathbb{M}_{init} as a_j
- 3: $A \leftarrow A \cup a_j$
- 4: **while** not COMPLETED **do**
- 5: $j = j + 1$
- 6: **while** VIOLATED **do**
- 7: Randomly select a module from $\mathbb{M} \setminus \mathbb{M}_{\text{init}}$ as a_j
- 8: Check the violation between a_j and a_{j-1}
- 9: **end while**
- 10: $A \leftarrow A \cup a_j$
- 11: **end while**

control policy (typically denoted as the meta-level policy π_θ) to automatically dictate desired configuration for EAs (Ma et al. 2024b; Yang, Wang, and Li 2024). Generally speaking, the workflow of MetaBBO follows a bi-level optimization process: 1) At the meta level, the policy π_θ configures the low-level EA and assesses its performance, termed meta performance. The policy leverages this observed meta performance to refine its decision-making process, training itself through the maximization of accumulated meta performance, thereby advancing its meta objective. 2) At the lower level, the BBO algorithm receives a designated algorithmic configuration from the meta policy. With this configuration in hand, the low-level algorithm embarks on the task of optimizing the target objective. It observes the changes in the objective values and relays this information back to the meta optimizer, contributing to the meta performance signal. Similarly, existing MetaBBO works focus predominantly on OS and PC. Although a predefined operator group remains necessary, the selection decisions in works on OS (Sharma et al. 2019; Tan and Li 2021; Lian et al. 2024) are made by the meta policy π_θ which relieves

the expert-level knowledge requirement. A notable example is RL-DAS (Guo et al. 2024) where advanced DE algorithms are switched entirely for complementary performance. In PC scenarios, initial works parameterize π with simple Multi-Layer Perceptron (MLP) (Wu and Wang 2022; Tan et al. 2022) and Long Short-Term Memory (LSTM) (Sun et al. 2021), whereas the latest work GLEET (Ma et al. 2024a) employs Transformer (Vaswani et al. 2017) architecture aiming at more versatile configuration. Besides, works jointly configure both OS and PC such as MADAC (Xue et al. 2022) also show robust performance on complex problems (Eimer et al. 2021).

3 Methodology

In this section, we elaborate on ConfigX step by step. We first explain in Section 3.1 the design of Modular-BBO and how to use it for efficient generation of diverse algorithm structures. We next provide a Markov Decision Process (MDP) definition of an optimization task and derive the corresponding multi-task learning objective in Section 3.2. At last, we introduce in Section 3.3 the details of each component in the defined MDP and the proposed Transformer based architecture.

3.1 Modular-BBO

As illustrated in the left of Figure 2, the design philosophy of Modular-BBO adheres to a Hierarchical Polymorphism in *Python* which ensures the ease of maintaining different sub-modules (third-level sub-classes in Figure 2, labeled in green), as well as their practical variants (bottom-level sub-classes in Figure 2, labeled in red) in modern EAs. By facilitating the high-to-low level inheritances, Modular-BBO provides universal programming interfaces for the modularization of EAs, along with essential module-specific properties/methods to support diverse behaviours of various sub-modules. Further elaboration on each inheritance level is

provided below.

High-level. All sub-module classes in Modular-BBO stem from an abstract base class `MODULE`. It declares universal properties/interfaces shared among various sub-module variants, yet leave them void. At high-level inheritance, two sub-classes `UNCONTROLLABLE` and `CONTROLLABLE` inherit from `MODULE`. The two sub-classes divide all possible sub-modules in modern EAs into the ones with (hyper-) parameters and those without. For `CONTROLLABLE` modules, we declare its (hyper-) parameters by adding a *config_space* property. Additionally, we include the corresponding *get_config()* and *set_config()* methods for configuring the (hyper-) parameters. Currently, these properties and methods remain void until a specific EA sub-module is instantiated.

Middle-level. At this inheritance level, `UNCONTROLLABLE` and `CONTROLLABLE` are further divided into common sub-modules in EAs, e.g., initialization, mutation, selection and etc.. Modular-BBO aims at generating legal algorithm structure via the combination of these sub-modules. When inheriting from either `UNCONTROLLABLE` or `CONTROLLABLE`, we introduce module-specific *topology_rule* as a guidance during the generating process (Algorithm 1), by invoking the added *get_rule()* method. We present a pair of examples in the left of Figure 2 to showcase one of the possible violation during the algorithm structure generation, where `CROSSOVER` is not allowed after `SELECTION` is a common sense in EAs.

Low-level. Within the low-level inheritance, we borrow from a large body of EA literature diverse practical sub-module variants (i.e., lots of initialization strategy have been proposed in literature such as Sobol sampling (Sobol 1967) and LHS sampling (McKay, Beckman, and Conover 2000)) and maintaining them by inheriting from the sub-module classes in middle-level inheritance. When inheriting from the parent class, a concrete sub-module variant has to specify its module *id* and *config_space*, which detail its unique identifier in Modular-BBO and controllable parameters respectively. It also have to overload *exec()* method by which it operates the solution population. The unique module id of a sub-module variant is a 16-bit binary code of which: 1) the first bit is 0 or 1 to denote if this variant is `UNCONTROLLABLE` or `CONTROLLABLE`. 2) the 2-nd to 7-th bits denote the sub-module category (third-level sub-classes in Figure 2, labeled in green) to which the variant belongs. 3) the last 9 bits denotes its id within this sub-module category.

For now, Modular-BBO has included 11 common sub-module categories in EAs: `INITIALIZATION` (Kazimipour, Li, and Qin 2014), `MUTATION` (Das, Mullick, and Suganthan 2016), `CROSSOVER` (Spears 1995), `PSO_UPDATE` (Shami et al. 2022), `BOUNDARY_CONTROL` (Kadavy et al. 2023), `SELECTION` (Shukla, Pandey, and Mehrotra 2015), `MULTI_STRATEGY` (Gong et al. 2011), `NICHING` (Ma et al. 2019), `INFORMATION_SHARING` (Toulouse, Crainic, and Gendreau 1996), `RESTART_STRATEGY` (Jansen 2002), `POPULATION_REDUCTION` (Pool and Nielsen 2007). We construct a collection of over 100 variants for these sub-module

categories from a large body of literature and denote this collection as module space \mathbb{M} . Theoretically, by using the algorithm generation process described in Algorithm 1, Modular-BBO spans a massive algorithm structure space \mathcal{A} containing millions of algorithm structures. Due to the limitation of space, we provide the detail of each sub-module variant in \mathbb{M} in Appendix A, Table 1, including the id, name, type, configuration space, topology rule and functional description. We also provide a detailed explanation for Algorithm 1 in Appendix B.

3.2 Multi-task Learning in ConfigX

Optimization Task Space We first define an optimization task space \mathcal{T} as a synergy of an algorithm space \mathcal{A} and an optimization problem set \mathcal{I} . Then an optimization task $T \in \mathcal{T}$ can be defined as $T : \{A \in \mathcal{A}, p \in \mathcal{I}\}$. In this paper, we adopt the algorithm space spanned by Modular-BBO as \mathcal{A} , and the problem instances from well-known CoCo-BBOB benchmark (Hansen et al. 2010), Protein-docking benchmark (Hwang et al. 2010) and HPO-B benchmark (Arango et al. 2021) as \mathcal{I} .

AC as an MDP For an optimization task $T : \{A, p\}$, we facilitate a Transformer based policy π_θ (detailed in Section 3.3) to dynamically dictate desired configuration for A to solve p . This configuration process can be formulated as an Markov Decision Process (MDP) $\mathcal{M} := (S, C, \Gamma, R, H, \gamma)$, where S denotes the state space that reflect optimization status, C denotes the action space which is exactly the configuration space of algorithm A , $\Gamma(s_{t+1}|s_t, c_t)$ denotes the optimization transition dynamics, $R(s_t, c_t)$ measures the single step optimization improvement obtained by using configuration c_t for optimizing p . H and γ are the number of optimization iterations and discount factor respectively. At each optimization step t , the policy π_θ receives a state s_t and then outputs a configuration $c_t = \pi_\theta(s_t)$ for A . Using c_t , algorithm A optimizes the optimization problem p for a single step. The goal is to find an optimal policy π_{θ^*} which maximizes the accumulated optimization improvement during the optimization process: $G = \sum_{t=1}^H \gamma^{t-1} R(s_t, c_t)$. Recall that our ConfigX aims at addressing a more challenging objective in Eq. (2), where the goal is to maximize the accumulated optimization improvement G of all tasks $T \in \mathcal{T}$. We use s_t^i and c_t^i to denote the input state and the outputted configuration of the policy π_θ for the i -th task in \mathcal{T} . Then the objective in Eq. (2) can be rewritten as a multi-task RL problem:

$$\mathbb{J}(\theta) = \frac{1}{K \cdot N} \sum_{i=1}^{K \cdot N} \sum_{t=1}^H \gamma^{t-1} R(s_t^i, c_t^i) \quad (3)$$

where we sample $K \cdot N$ tasks from \mathcal{T} to train π_θ since the number of tasks in \mathcal{T} is massive. These tasks is sampled first by calling Algorithm 1 K times to obtain K algorithm structures, and then combine these algorithm with the N problem instances in \mathcal{I} . In this paper we use Proximal Policy Optimization (PPO) (Schulman et al. 2017), a popular policy gradient (Williams 1992) method for optimizing this objective in a joint policy optimization (Gupta et al. 2022) fashion. We include the pseudocode of the RL training in Appendix D.

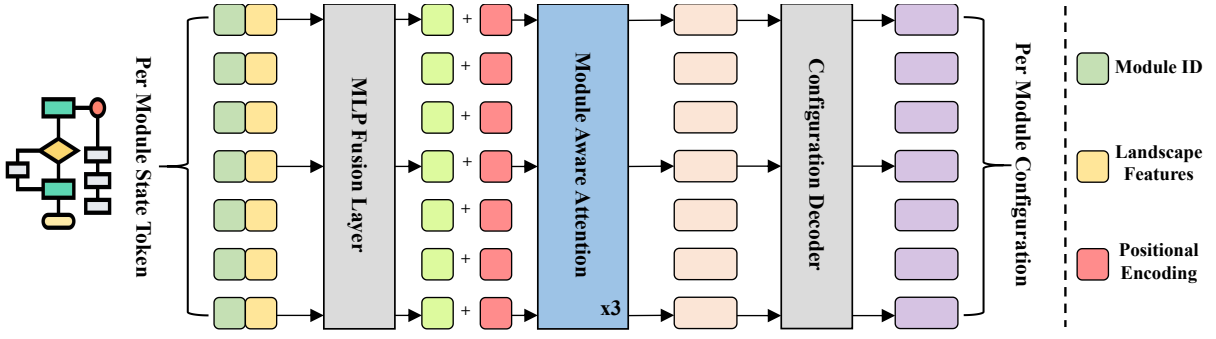


Figure 3: The workflow of the Transformer based configuration policy in ConfigX.

3.3 ConfigX

Progress in MetaBBO has made it possible to meta-learn neural network-based control policies for configuring the backbone EAs to solve optimization problems. However, existing MetaBBO methods are not suitable for the massive algorithm structure space \mathcal{A} spanned by the module space \mathbb{M} in our proposed Modular-BBO, since learning a separate policy for each algorithm structure is impractical. However, the modular nature of EAs implies that while each structure is unique, they are still constructed from the same module space and potentially shares sub-modules and workflows with other algorithm structures. We now describe how ConfigX exploits this insight to address the challenge of learning a universal controller for different algorithm structures.

State Design In ConfigX, we encode not only the algorithm structure information but also the optimization status information into the state representation to ensure the generalization across optimization tasks. Concretely, as illustrated in the left of Figure 3, for i -th tasks $T_i : \{A_i, p_i\}$ in the sampled $K \cdot N$ tasks, we encode a information pair for each sub-module in A_i , e.g., $s_i : \{s_{i,j}^{\text{id}}, s_{i,j}^{\text{opt}}\}_{j=1}^{L_i}$, where $s_{i,j}^{\text{id}} \in \{0, 1\}^{16}$ denotes the unique module id for j -th sub-module in A_i , $s_{i,j}^{\text{opt}} \in \mathbb{R}^9$ denotes the algorithm performance information which we borrow the idea from recent MetaBBO methods (Guo et al. 2024; Ma et al. 2024a), L_i denotes the number of sub-modules in A_i . We provide details of these information pairs in Appendix C.

State Encode We apply an MLP fusion layer to preprocess the state representation s_i . This fusion process ensures the information within the information pair $\{s_{i,j}^{\text{id}}, s_{i,j}^{\text{opt}}\}$ join each other smoothly (as illustrated in left part of Figure 3).

$$\begin{aligned} \hat{e}_{i,j} &= \text{hstack}(\phi(s_{i,j}^{\text{id}}; \mathbf{W}_e^{\text{id}}); \phi(s_{i,j}^{\text{opt}}; \mathbf{W}_e^{\text{opt}})) \\ e_{i,j} &= \phi(\hat{e}_{i,j}; \mathbf{W}_e), \quad j = 1, \dots, L_i \end{aligned} \quad (4)$$

Where $\phi(\cdot; \mathbf{W}_e^{\text{id}})$, $\phi(\cdot; \mathbf{W}_e^{\text{opt}})$ and $\phi(\cdot; \mathbf{W}_e)$ denotes MLP layers with the shape of 16×16 , 9×16 and 32×64 respectively, $e_{i,j}$ denotes the fused information for each sub-module. Then we add *Sin* Positional Encoding (Vaswani et al. 2017) \mathbf{W}_{pos} to each sub-module, which represents the relative position information among all sub-modules in the

algorithm structure.

$$\mathbf{h}_i^{(0)} = \text{vstack}(e_{i,j}; \dots; e_{i,L_i}) + \mathbf{W}_{\text{pos}} \quad (5)$$

where $\mathbf{h}_i^{(0)} \in \mathbb{R}^{L_{\max} \times 64}$ denotes the module embedding for each sub-module. We note that since the number of sub-modules (L_i) may vary between different algorithm structures, we zero pad $\mathbf{h}_i^{(0)}$ to a pre-defined maximum length L_{\max} to ensure input size invariant among tasks.

Module Aware Attention From the module embeddings $\mathbf{h}_i^{(0)}$ described above, we obtains the output features for all sub-modules as:

$$\begin{aligned} \hat{\mathbf{h}}_i^{(l)} &= \text{LN}(\text{MSA}(\mathbf{h}_i^{(l-1)}) + \mathbf{h}_i^{(l-1)}), \quad l = 1, 2, 3 \\ \mathbf{h}_i^{(l)} &= \text{LN}(\phi(\hat{\mathbf{h}}_i; \mathbf{W}_F^{(l)}) + \hat{\mathbf{h}}_i^{(l)}), \quad l = 1, 2, 3 \end{aligned} \quad (6)$$

where LN is Layernorm (Ba, Kiros, and Hinton 2016), MSA is Multi-head Self-Attention (Vaswani et al. 2017) and $\phi(\cdot; \mathbf{W}_F^{(l)})$ are MLP layers with the shape of 64×64 . In this paper we use $l = 3$ MSA blocks to process the module embeddings (as illustrated in the middle of Figure 3).

Configuration Decoder In ConfigX, the policy $\pi_{\theta}(c_i | s_i)$ models the conditional distribution of A_i 's configuration c_i given the state s_i . As illustrated in the right of Figure 3, for each sub-module a_j in an algorithm $A_i = \{a_1, a_2, \dots\}$, we output distribution parameters μ and Σ as:

$$\begin{aligned} \mu_j &= \phi(h_{i,j}^{(3)}; \mathbf{W}_{\mu}), \quad \Sigma_j = \text{Diag}(\phi(h_{i,j}^{(3)}; \mathbf{W}_{\Sigma})) \\ c_{i,j} &\sim \mathcal{N}(\mu_j; \Sigma_j) \end{aligned} \quad (7)$$

where $\phi(\cdot; \mathbf{W}_{\mu})$ and $\phi(\cdot; \mathbf{W}_{\Sigma})$ are two MLP layers with the same shape of $64 \times C_{\max}$, $c_{i,j} \in \mathbb{R}^{C_{\max}}$ denotes the configurations for sub-module a_j in algorithm structure A_i . Since the size of the configuration spaces may vary between different sub-modules, we pre-defined a maximum configuration space size C_{\max} to cover the sizes of all sub-modules. If the size of a sub-module is less than C_{\max} , we use the first few configurations in $c_{i,j}$ and ignore the rest.

For the critic, we calculate the value of a sub-module as $V(s_{i,j}) = \phi(\mathbf{h}_{i,j}^{(3)}; \mathbf{W}_c)$ using a MLP with the shape of $\mathbf{W}_c \in \mathbb{R}^{64 \times 16 \times 1}$. The value of the algorithm structure is the averaged value per sub-module $V(s_i) = \frac{1}{L_{\max}} \sum_{j=1}^{L_{\max}} V(s_{i,j})$.

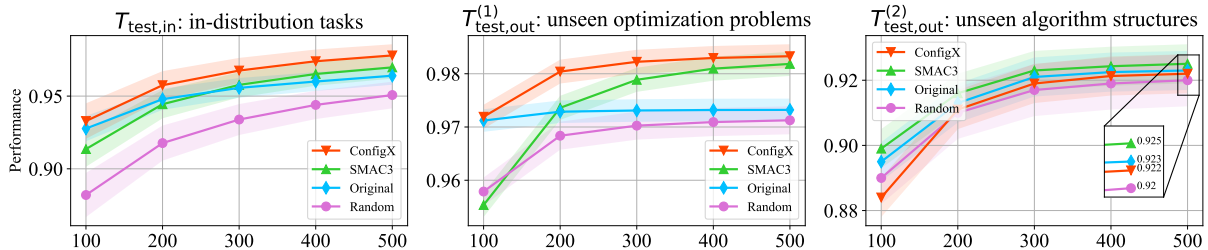


Figure 4: Optimization curves of the pre-trained ConfigX model and the baselines, over three different zero-shot scenarios.

Reward Function The objective value scales across different problem instances can vary. To ensure the accumulated performance improvement across tasks approximately share the same numerical level, we propose a task agnostic reward function. At optimization step t , the reward function on any problem instance $p \in \mathcal{I}$ is formulated as:

$$r_t = \delta \times \frac{f_{p,t-1}^* - f_{p,t}^*}{f_{p,0}^* - f_p^*} \quad (8)$$

where $f_{p,t}^*$ is the found best objective value of problem instance p at step t , f_p^* is the global optimal objective value of p and $\delta = 10$ is a scale factor. In this way, we make the scales of the accumulated improvement in all tasks similar and hence stabilize the training.

4 Experiment

In this section, we discuss the following research questions: **RQ1**: Can pre-trained ConfigX model zero-shots to unseen tasks with unseen algorithm structures and/or unseen problem instances? **RQ2**: If the zero-shot performance is not as expected, is it possible to fine-tune ConfigX to address novel algorithm structures in future? **RQ3**: How do the concrete designs in ConfigX contribute to the learning effectiveness? Below, we first introduce the experimental settings and then address RQ1~RQ3 respectively.

4.1 Experimental Setup

Training setup. We have prepared several task sets from different sub-task-spaces of the overall task space \mathcal{T} (defined at Section 3.2) to aid for the following experimental validation. Concretely, denote \mathcal{I}_{syn} as the problems in CoCo-BBOB suite, $\mathcal{I}_{\text{real}}$ as all realistic problems in Protein-docking benchmark and HPO-B benchmark, \mathcal{A}_{DE} as the algorithm structure space only including DE variants, $\mathcal{A}_{\text{PSO,GA}}$ as the algorithm structure space including PSO and GA variants, we have prepared 256 optimization tasks as training task set $T_{\text{train}} \subset \mathcal{A}_{\text{DE}} \times \mathcal{I}_{\text{syn}}$, another 512 optimization tasks as in-distribution testing task set $T_{\text{test,in}} \subset \mathcal{A}_{\text{DE}} \times \mathcal{I}_{\text{syn}}$. For out-of-distribution tasks, we have prepared two task sets: $T_{\text{test,out}}^{(1)} \subset \mathcal{A}_{\text{DE}} \times \mathcal{I}_{\text{real}}$ and $T_{\text{test,out}}^{(2)} \subset \mathcal{A}_{\text{PSO,GA}} \times \mathcal{I}_{\text{syn}}$, each with 512 task instances. During the training, for a batch of $\text{batch_size} = 32$ tasks, PPO (Schulman et al. 2017) method is used to update the policy net and critic $\kappa = 3$ times for every 10 rollout optimization steps. All of the optimization tasks are allowed to be optimized for $H = 500$ optimization

steps. The training lasts for 50 epochs with a fixed learning rate 0.001. All experiments are run on an Intel(R) Xeon(R) 6348 CPU with 504G RAM. Refer to Appendix E.1 for more details.

Baselines and Performance Metric. In the following comparisons, we consider three baselines: **SMAC3**, which is the state-of-the-art AC software based on Bayesian Optimization and aggressive racing mechanism; **Original**, which denotes using the suggested configurations in sub-modules' original paper (see Appendix A for one-to-one correspondence); **Random**, which randomly sample the configurations for the algorithm from the algorithm's configuration space. For the pre-trained model in ConfigX and the above baselines, we calculate the performance of them on tested task set by applying them to configure each tested task for 51 independent runs and then aggregate a normalized accumulated optimization improvement across all tasks and all runs, we provide more detailed calculation steps in Appendix E.2.

4.2 Zero-shot Performance (RQ1)

We validate the zero-shot performance of ConfigX by first pre-training a model on T_{train} . Then the pre-trained model is directly used to facilitate AC process for tasks in tested set, without any fine-tuning. Concretely, we aims at validating the zero-shot generalization performance in three different scenarios: 1) $T_{\text{test,in}}$, where the optimization tasks come from the same task space on which ConfigX is pre-trained. 2) $T_{\text{test,out}}^{(1)}$, where the optimization tasks locate beyond the optimization problem scope of the training task space. 3) $T_{\text{test,out}}^{(2)}$, where the optimization tasks locate beyond the algorithm structure scope of the training task space. We present the optimization curves of our pre-trained model and the baselines in Figure 4, where the x-axis denotes the optimization horizon and y-axis denotes the performance metric we defined previously. The results in Figure 4 reveal several key observations: 1) In all zero-shot scenarios, ConfigX presents significantly superior performance to the Random baseline, which randomly configures the algorithms in the tested tasks. This underscores the effectiveness of the multi-task reinforcement learning in ConfigX. 2) The results on $T_{\text{test,in}}$ demonstrate that pre-training ConfigX on some task samples of the given task space is enough to ensure the generalization to the other tasks within this space, surpassing the state-of-the-art AC baseline SMAC3. 3) The results on $T_{\text{test,out}}^{(1)}$ show that ConfigX is capable of adapting itself to to-

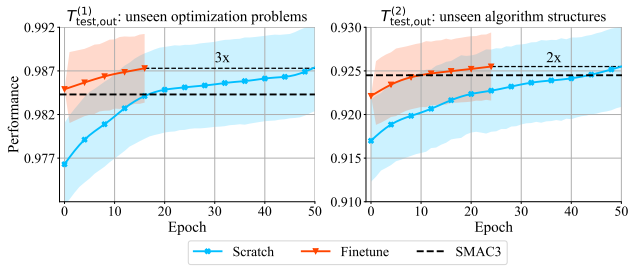


Figure 5: The learning curves of fine-tuning and re-training ConfigX on novel optimization problems or algorithm structures. The fine-tuning saves 3x and 2x learning steps than the re-training on $T_{\text{test,out}}^{(1)}$ and $T_{\text{test,out}}^{(2)}$ respectively.

tally unseen optimization problem scope. This observation attributes to our state representation design, where the optimization status borrowed from recent MetaBBO works are claimed to be generic across different problem scopes. 4) Though promising, we find that the zero-shot performance of ConfigX on $T_{\text{test,out}}^{(2)}$ is not as expected. It is not surprising as the sub-modules and structures in GA/PSO are significantly different from those in DE, which hinders ConfigX from applying its configuration experience with DE on PSO/GA optimization tasks. We explore whether this generalization gap could be addressed through further fine-tuning in the next section.

4.3 Lifelong Learning in ConfigX (RQ2)

The booming algorithm designs in EAs, together with the increasingly diverse optimization problems pose non-negligible challenges to universal algorithm configuration methods such as our ConfigX. On the one hand, although our pre-trained model shows uncommon AC performance when encountered with novel optimization problems (middle of Figure 4), further performance boost is still needed especially in industrial scenarios. On the other hand, as shown in the left of Figure 4, the pre-trained model can not cover those algorithm sub-modules which have not been included within its training algorithm structure space. Both situations above underline the importance of lifelong learning in ConfigX. We hence investigate the fine-tuning efficiency of the pre-trained model in this section. Concretely, we compare the learning curves of 1) fine-tuning the pre-trained model, and 2) re-training a new model from scratch in Figure 5, where the x-axis denotes the learning epochs and the y-axis denotes the aforementioned performance metric over the tested task set. The results reveal that ConfigX supports efficient fine-tuning for adapting out-of-distribution optimization tasks, which in turn provides operable guidance for lifelong learning in ConfigX: (a) One can configure an algorithm already included in the algorithm structure space of our Modular-BBO, yet on different problem scope, by directly using the pre-trained model. (b) One can also integrate novel algorithm designs into Modular-BBO and then facilitate efficient fine-tuning to enhance the performance of the pre-trained model on these novel algorithm structures.

| | $T_{\text{test,in}}$ | $T_{\text{test,out}}^{(1)}$ | $T_{\text{test,out}}^{(2)}$ |
|-------------|--|--|--|
| ConfigX | 9.81E-01 $\pm 7.33\text{E-}03$ | 9.86E-01 $\pm 2.64\text{E-}03$ | 9.22E-01 $\pm 6.94\text{E-}03$ |
| ConfigX-MLP | 9.70E-01 $\pm 8.13\text{E-}03$ | 9.80E-01 $\pm 2.54\text{E-}03$ | 9.16E-01 $\pm 6.57\text{E-}03$ |
| ConfigX-LPE | 9.82E-01 $\pm 7.62\text{E-}03$ | 9.84E-01 $\pm 2.58\text{E-}03$ | 9.20E-01 $\pm 6.89\text{E-}03$ |
| ConfigX-NPE | 9.74E-01 $\pm 7.75\text{E-}03$ | 9.81E-01 $\pm 2.67\text{E-}03$ | 9.19E-01 $\pm 6.73\text{E-}03$ |
| MLP-NPE | 9.51E-01 $\pm 9.27\text{E-}03$ | 9.73E-01 $\pm 2.71\text{E-}03$ | 9.06E-01 $\pm 7.29\text{E-}03$ |

Table 1: Performance of different ablated baselines.

4.4 Ablation Study (RQ3)

In Section 3.3, we proposed a Transformer based architecture to encode and process the state information of all sub-modules within an algorithm structure. In particular, we added *Sin* positional embeddings (PE) to each sub-module token as additional topology structure information for learning. We further apply Multi-head Self-Attention (MSA) to enhance the module-aware information sharing. In this section we investigate on what extent these designs influence ConfigX’s learning effectiveness. Concretely, for the positional embeddings, we introduce two ablations 1) ConfigX-NPE: remove the *Sin* PE from ConfigX. 2) ConfigX-LPE, replace the *Sin* PE by Learnable PE (Gehring et al. 2017). For the MSA, we introduce one ablation ConfigX-MLP: cancel the information sharing between the sub-modules by replacing the MSA blocks by an MLP layer. We present the final performance of these baselines and ConfigX on the tested task sets in Table 1. The results underscores the importance of these special designs: (a) Without the MSA block, ConfigX struggles in learning the configuration policy in an informative way. (b) Without the positional embeddings, the configuration policy in ConfigX becomes agnostic to the structure information of the controlled algorithm. (c) Learnable PE shows similar performance with *Sin* PE, while introducing additional parameters for ConfigX to learn.

5 Conclusion

In this paper, we propose ConfigX as a pioneer research exploring the possibility of learning a universal MetaBBO agent for automatically configuring diverse EAs across optimization problems. To this end, we first introduce a novel EA modularization system Modular-BBO that is capable of maintaining various sub-modules in EAs and spanning a massive algorithm structure space. We then formulate the universal AC over this algorithm space as an MTRL problem and hence propose meta-learning a Transformer based configuration policy to maximize the overall optimization performance across task samples. Extensive experiments demonstrate that a pre-trained ConfigX model could achieve superior AC performance to the state-of-the-art manual AC method SMAC3. Furthermore, we verify that ConfigX holds promising lifelong learning ability when being fine-tuned to adapt out-of-scope algorithm structures and optimization problems. We hope this work could serve as a pivotal step towards automatic and all-purpose AC base model.

6 Acknowledgments

This work was supported in part by the National Natural Science Foundation of China under Grant 62276100, in part by the Guangdong Natural Science Funds for Distinguished Young Scholars under Grant 2022B1515020049, and in part by the TCL Young Scholars Program.

A List of Sub-modules

We provide a complete list of the UNCONTROLLABLE and CONTROLLABLE sub-modules included in Modular-BBO in Table 2 and Table 3 respectively, where the module types, concrete variants’ names, functional descriptions, configuration space (only for CONTROLLABLE) and topology rules are presented. The configuration space description for each sub-module variant includes not only its legal value space but also its default value in the original paper. The topology rule of each sub-module variant, which contains a list of sub-module types, provides an information for algorithm structure generation procedure about which type of sub-modules can not be placed after this sub-module variant. Specially, we have only showcased a few MULTI_STRATEGY sub-module variants in the table due to the space limitation. For a MULTI_STRATEGY sub-module, it holds a more complicated configuration space than the others since it is an ensemble of other simple sub-module variants. When it shows up in a generated algorithm structure, our ConfigX has to select a sub-module variant in its ensemble first and configure the corresponding hyper-parameters at the same time.

B Algorithm Structure Generation

The actual algorithm structure generation procedure in Modular-BBO follows the Algorithm 1 in the main body. It always starts with randomly selecting an INITIALIZATION sub-module variant. Given the selected initialization variant, the next sub-module which follows is decided by checking the **COMPLETED** and **VIOLATED** conditions. In such case, for the currently selected one, we first check the topology rule list of the it. If the randomly selected follower is not in this list, **VIOLATED** is set to *true*, else *false*. When an legal follower is selected, we check the **COMPLETED** condition by simply checking if it is a **COMPLETED** sub-module, which is specially designed by us to denote the end of an algorithm structure (see the last row in Table 2). Specially, to select a legal subsequent sub-module variant for NICHING sub-module, it would introduce several branches to represent multi-sub-population algorithm structure. Hence, the following generation of NICHING sub-module is separated into branches. For each branch (sub-population), we follow the same selection procedure until a **COMPLETED** sub-module is selected for the corresponding branch. To summarize, bounded by these two conditions, the algorithm structure generation procedure ensures that: (a) all possible algorithm structures follow the common sense in regular EAs. (b) the sub-modules of different EA types will not appear together in a legal algorithm structure.

C State Details

In Section 3.3 of the paper, we encode a information pair for the j -th sub-module in algorithm \mathcal{A}_i as $s_{i,j} : \{s_{i,j}^{\text{id}}, s_{i,j}^{\text{opt}}\}$. Here $s_{i,j}^{\text{id}} \in \{0, 1\}^{16}$ is the 16 bit binary module id presented in Table 2 and Table 3. The algorithm performance information $s_i^{\text{opt}} \in \mathbb{R}^9$ contains 9 optimization features which are summarized below:

1. The first feature is the minimum objective value in the current (sub-)population indicating the achieved best performance of the current (sub-)population:

$$s_{i,1}^{\text{opt}} = \min\left\{\frac{f_i}{f_{0,*} - f^*}\right\}_{i \in [1, NP_{\text{local}}]} \quad (9)$$

It is normalized by the difference between the best objective value at initial optimization $f_{0,*}$ step and the global optimal objective value of the optimization problem f^* , so that the scales of the features from different tasks are in the same level. which hence stabilizes the training. NP_{local} is the (sub-)population size.

2. The second one is the averaged normalized objective values in the current (sub-)population, indicating the average performance of the (sub-)population:

$$s_{i,2}^{\text{opt}} = \text{mean}\left\{\frac{f_i}{f_{0,*} - f^*}\right\}_{i \in [1, NP_{\text{local}}]} \quad (10)$$

3. The variance of the normalized objective values in the current (sub-)population, indicating the variance and convergence of the (sub-)population:

$$s_{i,3}^{\text{opt}} = \text{std}\left\{\frac{f_i}{f_{0,*} - f^*}\right\}_{i \in [1, NP_{\text{local}}]} \quad (11)$$

4. The next feature is the maximal distance between the solutions in (sub-)population, normalized by the diameter of the search space, measuring the convergence:

$$s_{i,4}^{\text{opt}} = \max_{i,j \in [1, NP_{\text{local}}]} \frac{\|x_i - x_j\|_2}{\|ub - lb\|_2} \quad (12)$$

where ub and lb are the upper and lower bounds of the search space.

5. The dispersion difference (Lunacek and Whitley 2006) feature is calculated as the difference of the maximal distance between the top 10% solutions and the maximal distance between all solutions in (sub-)population:

$$s_{i,5}^{\text{opt}} = \max_{i,j \in [1, 10\% NP_{\text{local}}]} \frac{\|x_i - x_j\|_2}{\|ub - lb\|_2} - \max_{i,j \in [1, NP_{\text{local}}]} \frac{\|x_i - x_j\|_2}{\|ub - lb\|_2} \quad (13)$$

It measures the funnelity of the problem landscape: a single funnel problem has a smaller dispersion difference while the multi-funnel landscape has larger value.

6. The fitness distance correlation (FDC) (Tomassini et al. 2005) describes the complexity of the problem by evaluating the relationship between fitness value and the distance of the solution from the optimum.

$$s_{i,6}^{\text{opt}} = \frac{\frac{1}{NP_{\text{local}}} \sum_{i=1}^{NP_{\text{local}}} (f_i - \bar{f})(d_i^* - \bar{d}^*)}{\text{var}(\{d_i^*\}_{i \in [1, NP_{\text{local}}]}) \cdot \text{var}(\{f_i\}_{i \in [1, NP_{\text{local}}]})} \quad (14)$$

| type | Sub-module | | |
|----------------------|---|--|--|
| | Name + Id | Functional Description | Topology Rule |
| INITIALIZATION | Uniform (Kazimipour, Li, and Qin 2014) 0 - 0000001 - 000000001 | Uniformly sample solutions in the search range $x \sim U(lb, ub)$ where ub and lb are the upper and lower bounds of the search space. | Legal followers: DE-style MUTATION, PSO.UPDATE, GA-style CROSSOVER, MULTI_STRATEGY |
| | Sobol (Joe and Kuo 2008) 0 - 0000001 - 000000010 | Sample population in Sobol' sequences. | Legal followers: DE-style MUTATION, PSO.UPDATE, GA-style CROSSOVER, MULTI_STRATEGY |
| | LHS (McKay, Beckman, and Conover 2000) 0 - 0000001 - 000000011 | Sample population in Latin hypercube sampling. | Legal followers: DE-style MUTATION, PSO.UPDATE, GA-style CROSSOVER, MULTI_STRATEGY |
| | Halton (Halton 1960) 0 - 0000001 - 000000100 | Sample population in Halton sequence. | Legal followers: DE-style MUTATION, PSO.UPDATE, GA-style CROSSOVER, MULTI_STRATEGY |
| | Normal (Mahdavi, Rahnamayan, and Deb 2016) 0 - 0000001 - 000000101 | Sample solutions in Normal distribution $x \sim N((ub + lb)/2, \frac{1}{5}(ub - lb))$ where ub and lb are the upper and lower bounds of the search space. | Legal followers: DE-style MUTATION, PSO.UPDATE, GA-style CROSSOVER, MULTI_STRATEGY |
| NICHING | Rand (Liang and Suganthan 2005) 0 - 0000010 - 000000001 | Randomly partition the overall population into $N_{nich} \in [2, 4]$ same size sub-populations. | Legal followers: DE-style MUTATION, PSO.UPDATE, GA-style CROSSOVER, MULTI_STRATEGY |
| | Ranking (Arruda et al. 2008) 0 - 0000010 - 000000010 | Sort the population according to their fitness and partition them into $N_{nich} \in [2, 4]$ same size sub-populations. | Legal followers: DE-style MUTATION, PSO.UPDATE, GA-style CROSSOVER, MULTI_STRATEGY |
| | Distance (Liu et al. 2020) 0 - 0000010 - 000000011 | Randomly select a solution and assign its $NP/N_{nich} - 1$ nearest solutions to a new sub-population, until all solutions are assigned. | Legal followers: DE-style MUTATION, PSO.UPDATE, GA-style CROSSOVER, MULTI_STRATEGY |
| BOUNDARY_CONTROL | Clip (Kadavy et al. 2023) 0 - 0000011 - 000000001 | Clip the solutions out of bounds at the bound $x_i = \text{clip}(x_i, lb, ub)$ | Legal followers: SELECTION |
| | Rand (Kadavy et al. 2023) 0 - 0000011 - 000000010 | Randomly regenerate those out of bounds $x_{i,j} = \begin{cases} x_{i,j}, & \text{if } lb_j \leq x_{i,j} \leq ub_j, \\ U(lb_j, ub_j), & \text{otherwise} \end{cases}$ | Legal followers: SELECTION |
| | Periodic (Kadavy et al. 2023) 0 - 0000011 - 000000011 | Consider the search range as a closed loop $x_{i,j} = \begin{cases} x_{i,j}, & \text{if } lb_j \leq x_{i,j} \leq ub_j, \\ lb_j + ((x_{i,j} - ub_j) \bmod (ub_j - lb_j)), & \text{otherwise} \end{cases}$ | Legal followers: SELECTION |
| | Reflect (Kadavy et al. 2023) 0 - 0000011 - 000000100 | Reflect the values that hit the bound $x_{i,j} = \begin{cases} 2ub_j - x_{i,j}, & \text{if } ub_j < x_{i,j}, \\ 2lb_j - x_{i,j}, & \text{if } x_{i,j} < lb_j, \\ x_{i,j}, & \text{otherwise} \end{cases}$ | Legal followers: SELECTION |
| | Halving (Kadavy et al. 2023) 0 - 0000011 - 000000101 | Halve the distance between the x_i and the crossed bound $x_{i,j} = \begin{cases} x_{i,j} + 0.5 \cdot (x_{i,j} - ub_j), & \text{if } ub_j < x_{i,j}, \\ x_{i,j} + 0.5 \cdot (x_{i,j} - lb_j), & \text{if } x_{i,j} < lb_j, \\ x_{i,j}, & \text{otherwise} \end{cases}$ | Legal followers: SELECTION |
| SELECTION | DE-like (Storn and Price 1997) 0 - 000100 - 000000001 | Select the better one from the parent solution and its trail solution. | Legal followers: RESTART_STRATEGY, POPULATION_REDUCTION, COMPLETED, INFORMATION_SHARING (If NICHING is used) |
| | Crowding (Brest, Maučec, and Bošković 2021) 0 - 000100 - 000000010 | The trail solution compete against its closest solution and the better one survives. | Legal followers: RESTART_STRATEGY, POPULATION_REDUCTION, COMPLETED, INFORMATION_SHARING (If NICHING is used) |
| | PSO-like (Kennedy and Eberhart 1995) 0 - 000100 - 000000011 | Replace the old population with the new solutions without objective value comparisons. | Legal followers: RESTART_STRATEGY, POPULATION_REDUCTION, COMPLETED, INFORMATION_SHARING (If NICHING is used) |
| | Ranking (Baker 2014) 0 - 000100 - 000000100 | Select solutions for the next generation according to the ranking based probabilities, with the worst one ranking 1, the probability of the solution rank i is $p_i = \frac{1}{NP} (p^* + (p^* - p^-) \frac{i-1}{NP-1})$ where NP is the population size, p^* is the probability of selecting the best solution and p^- is the probability of selecting the worst one. | Legal followers: RESTART_STRATEGY, POPULATION_REDUCTION, COMPLETED, INFORMATION_SHARING (If NICHING is used) |
| | Tournament (Goldberg and Deb 1991) 0 - 000100 - 000000101 | Randomly pair solutions and select the better one in each pair for the next generation. | Legal followers: RESTART_STRATEGY, POPULATION_REDUCTION, COMPLETED, INFORMATION_SHARING (If NICHING is used) |
| | Roulette (Holland 1992) 0 - 000100 - 000000110 | Select solutions according to the fitness based probabilities $p_i = \frac{f_i}{\sum_{j=1}^{NP} f_j}$ where f_j is the fitness of the j -th solution and NP is population size. | Legal followers: RESTART_STRATEGY, POPULATION_REDUCTION, COMPLETED, INFORMATION_SHARING (If NICHING is used) |
| RESTART_STRATEGY | Stagnation (Peng et al. 2009) 0 - 000101 - 000000001 | Reinitialize the population if the improvement of the best objective value is equal to or less than a threshold 10^{-10} for 100 generations. | Legal followers: COMPLETED |
| | Obj_Convergence (Brest, Maučec, and Bošković 2021) 0 - 000101 - 000000010 | Reinitialize the population if the maximal difference of the objective values of the top 20% solutions is less than a threshold 10^{-16} . | Legal followers: COMPLETED |
| | Solution_Convergence (Zhabitskaya and Zhabitsky 2013) 0 - 000101 - 000000011 | Reinitialize the population if the maximal difference of the solutions on all dimensions are less than a threshold 10^{-16} search space diameter. | Legal followers: COMPLETED |
| | Obj&Solution_Convergence (Poláková, Tvrđík, and Bujok 2014) 0 - 000101 - 000000100 | Reinitialize the population if the maximal difference of the objective values is less than threshold 10^{-8} and the maximal distance among solutions is less than 0.005 search space diameter. | Legal followers: COMPLETED |
| POPULATION_REDUCTION | Linear (Tanabe and Fukunaga 2014) 0 - 000110 - 000000001 | Linearly reduce the population size from the initial size NP_{max} to the minimal population size NP_{min} . The size at generation $g + 1$ is $NP_{g+1} = \text{round}((NP_{min} - NP_{max}) \cdot \frac{g}{H}) + NP_{max}$ where g is the generation number and H is the optimization horizon. | Legal followers: Restart_Strategy, COMPLETED |
| | Non-Linear (Stanovov, Akhmedova, and Semenkina 2021) 0 - 000110 - 000000010 | Non-linearly determine the $g + 1$ generation population size as $NP_{g+1} = \text{round}((NP_{min} - NP_{max})^{1-g/H} + NP_{max})$ where NP_{min} and NP_{max} are the minimal and maximal population sizes, g is the generation number and H is the optimization horizon. | Legal followers: Restart_Strategy, COMPLETED |
| COMPLETED | COMPLETED 0 - 000111 - 000000001 | A token indicating the completion of algorithm structure generation which has no practical function. | - |

Table 2: The list of the practical variants of UNCONTROLLABLE modules.

where the \bar{f} is the averaged objective value in (sub-)population, $d_i^* = \|x_i - x^*\|_2$ is the distance between x_i and the best solution x^* , $\bar{d}^* = \text{mean}\{d_i^*\}_{i \in [1, NP_{local}]}$ is the averaged distance, $\text{var}(\cdot)$ is the variance.

7. The found global best objective among all (sub-)populations, indicating the achieved best performance of the overall optimization:

$$s_{i,7}^{\text{opt}} = \min\left\{\frac{f_i}{f_{0,*} - f^*}\right\}_{i \in [1, NP]} \quad (15)$$

8. This feature is the FDC feature for the overall population:

$$s_{i,8}^{\text{opt}} = \frac{\frac{1}{NP} \sum_{i=1}^{NP} (f_i - \bar{f})(d_i^* - \bar{d}^*)}{\text{var}(\{d_i^*\}_{i \in [1, NP]}) \cdot \text{var}(\{f_i\}_{i \in [1, NP]})} \quad (16)$$

9. The last feature is the remaining optimization budget, indicating the optimization progress:

$$s_{i,9}^{\text{opt}} = \frac{H - t}{H} \quad (17)$$

where H is the optimization horizon and t is the current optimization step.

Feature 1~6 measures the local optimization status in the sub-population the sub-modules belonging to. If there is no Niching and only one population, these features measures the status of the global population. Features 7~9 describes the global optimization across sub-populations such as the global optimization progress and the remaining optimization budget. The combination of local and global optimization status provides agent comprehensive optimization information about the sub-modules and the tasks. Besides, these

| type | Name + Id | Functional Description | Sub-module | Configuration Space | Topology Rule |
|--|--|---|---|---|--|
| MUTATION | DE/rand/1 (Storn and Price 1997) 1 - 00001 - 000000001 | Generate solution x_i 's trail solution $v_i = x_{i-1} + F1 \cdot (x_{best} - x_{i-1})$ where x_{i-1} are randomly selected solutions. | | $F1 \in [0, 1]$, default to 0.5. | Legal followers: DE-style CROSSOVER, MULTI_STRATEGY |
| | DE/rand/2 (Storn and Price 1997) 1 - 00001 - 000000010 | Generate solution x_i 's trail solution by $v_i = x_{i-1} + F1 \cdot (x_{i-2} - x_{i-1}) + F2 \cdot (x_{i-1} - x_{i-2})$ where x_{i-1} are randomly selected solutions. | | $F1, F2 \in [0, 1]$, default to 0.5. | Legal followers: DE-style CROSSOVER, MULTI_STRATEGY |
| | DE/best/1 (Storn and Price 1997) 1 - 00001 - 000000001 | Generate solution x_i 's trail solution by $v_i = x_{best} + F1 \cdot (x_i - x_{best})$ where x_{i-1} are randomly selected solutions and x_{best} is the best solution. | | $F1 \in [0, 1]$, default to 0.5. | Legal followers: DE-style CROSSOVER, MULTI_STRATEGY |
| | DE/best/2 (Storn and Price 1997) 1 - 00001 - 000000100 | Generate solution x_i 's trail solution by $v_i = x_{best} + F1 \cdot (x_{i-1} - x_{best}) + F2 \cdot (x_{i-2} - x_{best})$ where x_{i-1} are randomly selected solutions and x_{best} is the best solution. | | $F1, F2 \in [0, 1]$, default to 0.5. | Legal followers: DE-style CROSSOVER, MULTI_STRATEGY |
| | DE/current-to-best/1 (Storn and Price 1997) 1 - 00001 - 000000101 | Generate solution x_i 's trail solution by $v_i = x_i + F1 \cdot (x_{best} - x_i) + F2 \cdot (x_{i-1} - x_{best})$ where x_{i-1} are randomly selected solutions and x_{best} is the best solution. | | $F1, F2 \in [0, 1]$, default to 0.5. | Legal followers: DE-style CROSSOVER, MULTI_STRATEGY |
| | DE/current-to-best/2 (Storn and Price 1997) 1 - 00001 - 000000110 | Generate solution x_i 's trail solution by $v_i = x_i + F1 \cdot (x_{i-1} - x_i) + F2 \cdot (x_{i-2} - x_{i-1})$ where x_{i-1} are randomly selected solutions. | | $F1, F2 \in [0, 1]$, default to 0.5. | Legal followers: DE-style CROSSOVER, MULTI_STRATEGY |
| | DE/rand-to-best/1 (Storn and Price 1997) 1 - 00001 - 000000111 | Generate solution x_i 's trail solution by $v_i = x_i + F1 \cdot (x_{best} - x_{i-1})$ where x_{i-1} are randomly selected solutions and x_{best} is the best solution. | | $F1 \in [0, 1]$, default to 0.5. | Legal followers: DE-style CROSSOVER, MULTI_STRATEGY |
| | DE/current-to-pbest/1 (Zhang and Sanderson 2009) 1 - 00001 - 000001000 | Generate solution x_i 's trail solution by $v_i = x_i + F1 \cdot (x_{pbest} - x_i) + F2 \cdot (x_{i-1} - x_{pbest})$ where x_{i-1} are randomly selected solutions and x_{pbest} is a randomly selected from the top p best solutions. | | $F1, F2 \in [0, 1]$, default to 0.5; $p \in [0, 1]$, default to 0.05. | Legal followers: DE-style CROSSOVER, MULTI_STRATEGY |
| | DE/current-to-pbest/1+archive (Zhang and Sanderson 2009) 1 - 00001 - 000001001 | Generate solution x_i 's trail solution by $v_i = x_i + F1 \cdot (x_{pbest} - x_i) + F2 \cdot (x_{i-1} - x_{pbest})$ where x_{i-1} is a randomly selected solutions, x_{pbest} is randomly selected from the union of the population and the archive which contains inferior solutions, x_{pbest} is a randomly selected solution from the top p best solutions. | | $F1, F2 \in [0, 1]$, default to 0.5; $p \in [0, 1]$, default to 0.05. | Legal followers: DE-style CROSSOVER, MULTI_STRATEGY |
| | DE/weighted-rand-to-pbest/1 (Biswas et al. 2021) 1 - 00001 - 000001010 | Generate solution x_i 's trail solution by $v_i = x_i + F1 \cdot x_{i-1} + F1 \cdot F2 \cdot (x_{pbest} - x_{i-1})$ where x_{i-1} are randomly selected solutions and x_{pbest} is the best solution. | | $F1, F2 \in [0, 1]$, default to 0.5; $p \in [0, 1]$, default to 0.05. | Legal followers: DE-style CROSSOVER, MULTI_STRATEGY |
| DE/current-to-rand/1+archive (Biswas et al. 2021) 1 - 00001 - 000001011 | Generate solution x_i 's trail solution by $v_i = x_i + F1 \cdot (x_{i-1} - x_i) + F2 \cdot (x_{i-2} - x_{i-1})$ where x_{i-1}, x_{i-2} are randomly selected solutions, x_{i-1} is randomly selected from the union of the population and the archive which contains inferior solutions. | | $F1, F2 \in [0, 1]$, default to 0.5. | Legal followers: DE-style CROSSOVER, MULTI_STRATEGY | |
| Gaussian_mutation (Holland 1992) 1 - 00001 - 000001100 | Generate a mutated solution of x_i by adding a Gaussian noise on each dimension $v_i = N(x_i, \sigma \cdot (ub - lb))$ where ub and lb are the upper and lower bounds of the search space. | | $\sigma \in [0, 1]$, default to 0.1 | Legal followers: BOUNDARY_CONTROL, MULTI_STRATEGY | |
| Polynomial_mutation (Dobnikar et al. 1999) 1 - 00001 - 000001101 | Generate a mutated solution of x_i as $v_i = \begin{cases} x_i + ((2u)^{\frac{1}{\gamma_m}} - 1)(x_i - lb), & \text{if } u \leq 0.5; \\ x_i + (1 - (2 - 2u)^{\frac{1}{\gamma_m}})(x_i - lb), & \text{if } u > 0.5. \end{cases}$ where $u \in [0, 1]$ is a random number, ub and lb are the upper and lower bounds of the search space. | | $\gamma_m \in [20, 100]$, default to 20. | Legal followers: BOUNDARY_CONTROL, MULTI_STRATEGY | |
| CROSSOVER | Binomial (Storn and Price 1997) 1 - 00001 - 000000001 | Randomly exchange values between parent solution x_i and the trail solution v_i to get a new solution: $u_{i,j} = \begin{cases} v_{i,j}, & \text{if } rand_j < Cr \text{ or } j = jrand \\ x_{i,j}, & \text{otherwise} \end{cases}$, $j = 1, \dots, D$ where $rand_j \in [0, 1]$ is a random number, $jrand \in [1, D]$ is a randomly selected index before crossover and D is the solution dimension. | | $Cr \in [0, 1]$, default to 0.9. | Legal followers: BOUNDARY_CONTROL, MULTI_STRATEGY |
| | Exponential (Storn and Price 1997) 1 - 00001 - 000000010 | Exchange a random solution segment between x_i and v_i to get a new solution: $u_{i,j} = \begin{cases} v_{i,j}, & \text{if } rand_k < Cr \text{ and } k \leq j \leq L + k \\ x_{i,j}, & \text{otherwise} \end{cases}$, $j = 1, \dots, D$ where $k \in [1, D]$ is a randomly selected start point for exchanging, $L \in [1, D - k]$ is a randomly determined exchange length, $rand_{k,j} \in [0, 1]^{L-k}$ is the random numbers from index k to j and D is the solution dimension. | | $Cr \in [0, 1]$, default to 0.9. | Legal followers: BOUNDARY_CONTROL, MULTI_STRATEGY |
| | qbest_Binomial (Islam et al. 2011) 1 - 00001 - 000000011 | Randomly exchange values between a solution x_i selected from the top p population and the trail solution v_i to get a new solution: $u_{i,j} = \begin{cases} v_{i,j}, & \text{if } rand_j < Cr \text{ or } j = jrand \\ x_{i,j}, & \text{otherwise} \end{cases}$, $j = 1, \dots, D$ where $rand_j \in [0, 1]$ is a random number, $jrand \in [1, D]$ is a randomly selected index before crossover and D is the solution dimension. | | $Cr \in [0, 1]$, default to 0.9; $p \in [0, 1]$, default to 0.5 | Legal followers: BOUNDARY_CONTROL, MULTI_STRATEGY |
| | qbest_Binomial+archive (Biswas et al. 2021) 1 - 00001 - 000000100 | Randomly exchange values between a solution x_i selected from the top p population+archive union and the trail solution v_i to get a new solution: $u_{i,j} = \begin{cases} v_{i,j}, & \text{if } rand_j < Cr \text{ or } j = jrand \\ x_{i,j}, & \text{otherwise} \end{cases}$, $j = 1, \dots, D$ where $rand_j \in [0, 1]$ is a random number, $jrand \in [1, D]$ is a randomly selected index before crossover and D is the solution dimension. | | $Cr \in [0, 1]$, default to 0.9; $p \in [0, 1]$, default to 0.18 | Legal followers: BOUNDARY_CONTROL, MULTI_STRATEGY |
| | SBX (Deb, Agrawal et al. 1995) 1 - 00001 - 000000101 | Generate child solution(s) v_i by $v_i = 0.5 \cdot [(1 + \beta)x_{p1} + (1 - \beta)x_{p2}]$ where $\beta = \begin{cases} (2u)^{\frac{1}{\gamma_m}} - 1, & \text{if } u \leq 0.5; \\ (1 - (2 - 2u)^{\frac{1}{\gamma_m}}), & \text{if } u > 0.5. \end{cases}$, $u \in [0, 1]$ is a random number, x_{p1} and x_{p2} are two randomly selected parents. | | $\gamma_m \in [20, 100]$, default to 20 | Legal followers: GA-style MUTATION, MULTI_STRATEGY |
| Aithmetic (Michalewicz 2013) 1 - 00001 - 000000101 | Generate child solution v_i by $v_i = (1 - \alpha) \cdot x_{p1} + \alpha \cdot x_{p2}$ where x_{p1} and x_{p2} are two randomly selected parents. | | $\alpha \in [0, 1]$, default to 0.5. | Legal followers: GA-style MUTATION, MULTI_STRATEGY | |
| PSO_UPDATE | Vanilla_PSO (Kennedy and Eberhart 1995) 1 - 00001 - 000000001 | Update solution x_i^t at generation t using $x_i^{t+1} = x_i^t + vel_i^t$ where velocity vector $vel_i^t = w \cdot vel_i^{t-1} + c1 \cdot rand_1 \cdot (pbest_i^t - x_i^t) + c2 \cdot rand_2 \cdot (gbest^t - x_i^t)$, $rand \in [0, 1]$ are random values, $pbest_i^t$ is the best solution x_i ever achieved, $gbest^t$ is the global best solution. | | $w \in [0.4, 0.9]$, default to 0.7; $c1, c2 \in [0, 2]$, default to 1.49445. | Legal followers: BOUNDARY_CONTROL, MULTI_STRATEGY |
| | FDR_PSO (Peram, Veenamachaneni, and Mohan 2003) 1 - 00001 - 000000010 | Update solution x_i^t at generation t using $x_i^{t+1} = x_i^t + vel_i^t$ where velocity vector $vel_i^t = w \cdot vel_i^{t-1} + c1 \cdot rand_1 \cdot (pbest_i^t - x_i^t) + c2 \cdot rand_2 \cdot (gbest^t - x_i^t) + c3 \cdot rand_3 \cdot (nbest_i^t - x_i^t)$, $rand \in [0, 1]$ are random values, $pbest_i^t$ is the best solution x_i ever achieved, $gbest^t$ is the global best solution and $nbest_i^t$ is the solution that maximizes the Fitness-Distance-Ratio $nbest_i^t = x_{i,j}^t$ which $j = \arg \max_{p \in [1, N], q \in [1, D]} \frac{f_i^t - f_j^t}{ x_{i,p}^t - x_{i,q}^t }$, $j = 1, \dots, D$, f denotes the objective values and D is solution dimension. | | $w \in [0.4, 0.9]$, default to 0.729; $c1, c2 \in [0, 2]$, default to 1; $c3 \in [0, 2]$, default to 2. | Legal followers: BOUNDARY_CONTROL, MULTI_STRATEGY |
| | CLPSO (Liang et al. 2006) 1 - 00001 - 000000011 | Update solution x_i^t at generation t using $x_i^{t+1} = x_i^t + vel_i^t$ where velocity vector $vel_i^t = w \cdot vel_i^{t-1} + c1 \cdot rand_1 \cdot (pbest_{f,j}^t - x_i^t) + c2 \cdot rand_2 \cdot (gbest^t - x_i^t)$, where $rand \in [0, 1]$ are random values, $gbest^t$ is the global best solution, $pbest_{f,j}^t = \begin{cases} pbest_{f,j}^t, & \text{if } rand_j > P_{ci}; \\ pbest_{f,j}^t, & \text{otherwise.} \end{cases}$, $j = 1, \dots, D$ is the ever achieved best solution of x_i or x_j which is randomly selected with fitness based tournament. | | $w \in [0.4, 0.9]$, default to 0.7; $c1, c2 \in [0, 2]$, default to 1.49445. | Legal followers: BOUNDARY_CONTROL, MULTI_STRATEGY |
| MULTI_STRATEGY | Multi_Niching_2 1 - 00100 - 000000001 | It contains RAND, RANKING and DISTANCE three niching methods with the same sub-population size $N_{nich} = 2$, its action is to select one of the three methods to conduct niching. | | $op \in \{\text{RAND, RANKING, DISTANCE}\}$, random selection in default; | Legal followers: DE-style MUTATION, PSO_UPDATE, GA-style CROSSOVER, MULTI_STRATEGY |
| | Multi_Niching_3 1 - 00100 - 000000010 | It contains RAND, RANKING and DISTANCE three niching methods with the same sub-population size $N_{nich} = 3$, its action is to select one of the three methods to conduct niching. | | $op \in \{\text{RAND, RANKING, DISTANCE}\}$, default to RAND. | Legal followers: DE-style MUTATION, PSO_UPDATE, GA-style CROSSOVER, MULTI_STRATEGY |
| | Multi_Niching_4 1 - 00100 - 000000011 | It contains RAND, RANKING and DISTANCE three niching methods with the same sub-population size $N_{nich} = 4$, its action is to select one of the three methods to conduct niching. | | $op \in \{\text{RAND, RANKING, DISTANCE}\}$, default to RAND. | Legal followers: DE-style MUTATION, PSO_UPDATE, GA-style CROSSOVER, MULTI_STRATEGY |
| | Multi_BC 1 - 00100 - 000000100 | It contains the five Boundary_Control methods CLIP, RAND, PERIODIC, REFLECT and HALVING, its action is to select one of the five methods. | | $op \in \{\text{CLIP, RAND, PERIODIC, REFLECT, HALVING}\}$, default to CLIP. | Legal followers: SELECTION |
| | Multi_Mutation_1 (Biswas et al. 2021) 1 - 00100 - 000000101 | Contains DE/current-to-pbest/1+archive, DE/current-to-rand/1+archive and DE/weighted-rand-to-best/1 three DE mutation sub-modules, its first configuration is to select one of the three mutations and the rest configurations are to configured the selected operator. | | $op \in \{\text{DE/CURRENT-TO-PBEST/1+ARCHIVE, DE/CURRENT-TO-RAND/1+ARCHIVE, DE/WEIGHTED-RAND-TO-BEST/1}\}$, random selection in default; $F1, F2 \in [0, 1]$, default to 0.5; $p \in [0, 1]$, default to 0.18. | Legal followers: DE-style CROSSOVER |
| | Multi_Mutation_2 (Wang, Cai, and Zhang 2011) 1 - 00100 - 000000110 | Contains DE/rand/1, DE/rand/2 and DE/current-to-rand/1 three DE mutation sub-modules. | | $op \in \{\text{DE/RAND/1, DE/RAND/2, DE/CURRENT-TO-RAND/1}\}$, random selection in default; $F1, F2 \in [0, 1]$, default to 0.5. | Legal followers: DE-style CROSSOVER |
| | Multi_Mutation_3 (Mallipeddi et al. 2011) 1 - 00100 - 000000111 | Contains DE/rand/1, DE/best/2 and DE/current-to-rand/1 three DE mutation sub-modules. | | $op \in \{\text{DE/RAND/1, DE/BEST/2, DE/CURRENT-TO-RAND/1}\}$, random selection in default; $F1, F2 \in [0, 1]$, default to 0.5. | Legal followers: DE-style CROSSOVER |
| | Multi_Crossover_1 (Biswas et al. 2021) 1 - 00100 - 000001000 | Contains Binomial and qbest_Binomial+archive two DE crossover sub-modules. | | $op \in \{\text{BINOMIAL, QBEST_BINOMIAL+ARCHIVE}\}$, random selection in default; $Cr \in [0, 1]$, default to 0.9. | Legal followers: BOUNDARY_CONTROL |
| | Multi_Crossover_2 (Peng et al. 2021) 1 - 00100 - 000001001 | Contains Binomial and Exponential two DE crossover sub-modules. | | $op \in \{\text{BINOMIAL, EXPONENTIAL}\}$, random selection in default; $Cr \in [0, 1]$, default to 0.9. | Legal followers: BOUNDARY_CONTROL |
| | Multi_PSO_1 (Lynn and Suganthan 2017) 1 - 00100 - 000001010 | Contains FDR_PSO and CLPSO two PSO update sub-modules. | | $op \in \{\text{FDR_PSO, CLPSO}\}$, random selection in default; $w \in [0.4, 0.9]$, default to 0.729; $c1, c2 \in [0, 2]$, default to 1; $c3 \in [0, 2]$, default to 2. | Legal followers: BOUNDARY_CONTROL |
| 50 more Multi-Strategies about Mutations, Crossovers and PSO_Updates are omitted here since they are too many to presenting them one by one. 1 - 00100 - 000001011 ~1 - 00100 - 00011101 | ... | | ... | ... | |
| INFORMATION_SHARING | Sharing 1 - 00010 - 000000001 | Receive the best solution from the target sub-population and replace the worst solution in current sub-population. | | $target \in [1, N_{nich}]$, random selection in default | Legal followers: POPULATION_REDUCTION, COMPLETED |

Table 3: The list of the practical variants of CONTROLLABLE modules.

features are generic across different problem scopes, which empower ConfigX the generalization ability across unseen problems.

D Pseudo Code

In this section to enhance the clarity and overall comprehension of the paper, we present the pseudo code for the RL training process in Algorithm 2.

In the pseudocode we omit the batch processing on tasks for better readability. For each training epoch and each train-

Algorithm 2: Pseudocode for the overall training.

Input: The training task set T_{train} , the ConfigX policy π_θ and critic V_ϕ , PPO parameters $nstep = 10$ and $\kappa = 3$

Output: A well-trained policy π_{θ^*} .

```

1: for epoch  $\leftarrow$  1 to 100 do
2:   for task env  $\in T_{\text{train}}$  do
3:     Initialize the transition memory  $MT \leftarrow \emptyset$ 
4:     Environment initialization  $s_1 \leftarrow env.init()$ 
5:     for  $t \leftarrow$  1 to  $H$  do
6:       Get the algorithm configuration  $a_t \leftarrow \pi_\theta(s_t)$ 
7:       Execute one optimization step with the given configuration  $s_{t+1}, r_t \leftarrow env.step(a_t)$ 
8:        $MT \leftarrow MT \cup \langle s_t, a_t, s_{t+1}, r_t \rangle$ 
9:       if  $\text{mod}(t, nstep) = 0$  then
10:        for  $k \leftarrow$  1 to  $\kappa$  do
11:          Update  $\theta$  and  $\phi$  using  $MT$  in PPO manner
12:        end for
13:        Clear memory  $MT \leftarrow \emptyset$ 
14:      end if
15:    end for
16:  end for
17: end for

```

ing task form the training task set T_{train} , we first initialize a memory to contain the transitions. Then we consider the task as a RL environment and initialize it, in which the optimization population is generated and evaluated to obtain the initial optimization state s_1 whose formulation is detailed in Appendix C. For each optimization step, the action (configuration) a_t is determined by the policy π_t according to the current state. The algorithm in the environment (task) then takes an optimization step with the given configuration and returns the next state s_{t+1} and the reward r_t . For each 10 optimization steps, the policy parameters are updated for $\kappa = 3$ steps in PPO manner using the collected transitions.

E Experiment

E.1 Experiment Setup

Optimization Benchmarks In this paper to construct \mathcal{I}_{syn} and $\mathcal{I}_{\text{real}}$ we introduce three optimization problem sets: BBOB testsuite (Hansen et al. 2010), Protein-docking benchmark (Hwang et al. 2010) and HPO-B benchmark (Arango et al. 2021).

- \mathcal{I}_{syn} . In this problem space we adopt the BBOB testsuite (Hansen et al. 2010) which contains 24 optimization problems with diverse properties including unimodal or multi-modal, separable or non-separable, adequate or weak global structure, etc.. In experiments we set the search space to $[-5, 5]^D$ and randomly select the dimension D of each problem from $\{5, 10, 20, 50\}$. Besides, for each problem we randomly introduce a offset $z \sim \mathcal{U}(-4, 4)$ to the optimal and then randomly generate a rotational matrix $M \in \mathbb{R}^{D \times D}$ to rotate the searching space. The yielded transformed problems $f(M^T(x - z))$ construct the problem instance space \mathcal{I}_{syn} .
- $\mathcal{I}_{\text{real}}$. For this problem space we combine two realistic problem benchmarks: Protein-docking bench-

mark (Hwang et al. 2010) and HPO-B benchmark (Arango et al. 2021).

- **Protein-docking benchmark** (Hwang et al. 2010) aims at minimizing the Gibbs free energy resulting from protein-protein interaction between a given complex and any other conformation. We formulate the objective as follows:

$$\min_x E_{\text{int}}(x, x_0) = \sum_i^{atoms} \sum_j^{atoms} E(x^i, x_0^j), \quad (18)$$

where $E(x^i, x_0^j)$ is the energy between any pair atoms of x and x_0 , and is defined as :

$$E_{i,j} = \begin{cases} \frac{q_i q_j}{\epsilon r_{i,j}} + \sqrt{\epsilon_i \epsilon_j} \left[\left(\frac{R_{i,j}}{r_{i,j}} \right)^{12} - \left(\frac{R_{i,j}}{r_{i,j}} \right)^6 \right], & \text{if } r_{i,j} < 7 \\ \frac{(r_{off} - f_{i,j})^2 (r_{off} + 2r_{i,j} - 3r_{on})}{(r_{off} - r_{on})^3}, & \\ \left\{ \frac{q_i q_j}{\epsilon r_{i,j}} + \sqrt{\epsilon_i \epsilon_j} \left[\left(\frac{R_{i,j}}{r_{i,j}} \right)^{12} - \left(\frac{R_{i,j}}{r_{i,j}} \right)^6 \right] \right\}, & \text{if } 7 \leq r_{i,j} \leq 9 \\ 0 & \text{if } r_{i,j} > 9 \end{cases} \quad (19)$$

All parameters and calculations are taken from the Charmm19 force field (MacKerell Jr et al. 1998). We select 8 protein-protein complexes from the benchmark and associate each complex with 10 different starting points, chosen from the top-10 start points identified by ZDOCK (Pierce et al. 2014). Consequently, the Protein-Docking testsuites in this paper comprise a total of 80 docking problem instances. It is important to note that we parameterize the search space as \mathbb{R}^{12} , which is a reduced dimensionality compared to the original protein complex (Cao and Shen 2020).

- **HPO-B benchmark** (Arango et al. 2021) includes a wide range of hyper-parameter optimization tasks for 16 different model types (e.g., SVM, XGBoost, etc.). These models have various search spaces ranging from $[0, 1]^2$ to $[0, 1]^{16}$. Each model is evaluated on several datasets, resulting in a total of 86 tasks. In this paper, we adopt the continuous version of HPO-B, which provides surrogate evaluation functions for time-consuming machine learning tasks to save evaluation time.

Algorithm Space Split We have leveraged the convenience provided by our proposed Modular-BBO to construct two different algorithm structure sub-spaces: \mathcal{A}_{DE} and $\mathcal{A}_{\text{PSO,GA}}$. This algorithm space split help us validate if ConfigX could generalize far beyond the algorithm space it has been trained on.

- \mathcal{A}_{DE} . In this algorithm structure sub-space, all possible algorithm structures are DE algorithms. To construct such DE algorithm space, we add additional constraints during the algorithm structure generation structure. Concretely, for UNCONTROLLABLE sub-modules, they are shared among different EA types hence can be selected without constraints. For CONTROLLABLE sub-modules, we only constraints the optional range within those related with DE.

- $\mathcal{A}_{\text{PSO,GA}}$. Same like \mathcal{A}_{DE} , except that for CONTROL-LABLE sub-modules, we only constraints the optional range within those related with PSO and GA.

Task Set Construction We provide multiple zero-shot generalization scenarios in experiments part to validate the zero-shot performance of ConfigX on in-distribution and out-of-distribution tasks. Concretely, we have prepared 4 task sets for the training and testing of ConfigX:

- T_{train} . A group of 256 tasks within the joint task space combining the DE algorithm sub-space and synthetic problem space: $T_{\text{train}} \subset \mathcal{A}_{\text{DE}} \times \mathcal{I}_{\text{syn}}$. Concretely, we generate 32 DE algorithms from \mathcal{A}_{DE} and select 8 problem instances from \mathcal{I}_{syn} .
- $T_{\text{test,in}}$. A group of 512 tasks within the joint task space combining the DE algorithm sub-space and synthetic problem space: $T_{\text{test,in}} \subset \mathcal{A}_{\text{DE}} \times \mathcal{I}_{\text{syn}}$. Concretely, we generate 32 DE algorithms from \mathcal{A}_{DE} and select 16 problem instances from \mathcal{I}_{syn} .
- $T_{\text{test,out}}^{(1)}$. A group of 512 tasks within the joint task space combining the DE algorithm sub-space and synthetic problem space: $T_{\text{test,out}}^{(1)} \subset \mathcal{A}_{\text{DE}} \times \mathcal{I}_{\text{real}}$. Concretely, we generate 32 DE algorithms from \mathcal{A}_{DE} and select 16 problem instances from $\mathcal{I}_{\text{real}}$, 8 from Protein-docking benchmark and 8 from HPO-B.
- $T_{\text{test,out}}^{(2)}$. A group of 512 tasks within the joint task space combining the PSO and GA algorithm sub-space and synthetic problem space: $T_{\text{test,out}}^{(2)} \subset \mathcal{A}_{\text{PSO,GA}} \times \mathcal{I}_{\text{syn}}$. Concretely, we generate 32 PSO and GA algorithms from $\mathcal{A}_{\text{PSO,GA}}$ and select 16 problem instances from \mathcal{I}_{syn} .

E.2 Baselines and Performance Metric

Baselines. In the experiment section in main paper, we consider three baselines: SMAC3, Original and Random.

- **SMAC3.** It is a Bayesian Optimization (Shahriari et al. 2015) based hyper-parameter optimization software, we consider it as a baseline of human-crafted state-of-the-art automatic configuration. We in the experiments called the exposed interface `samc.facade.AlgorithmConfigurationFacade()` to determine a single well-performing robust configuration for an algorithm in entire optimization process. This interface combines RandomForest surrogate model, logEI acquisition function and aggressive racing intensification mechanism to provide robust AC performance across many AutoML tasks. In the experiments, we allow SMAC3 to search for optimal configurations for each algorithm structure in \mathcal{A}_{DE} and $\mathcal{A}_{\text{PSO,GA}}$ on the 8 training problem instances in T_{train} . Then we apply the optimized configurations for the generalization performance evaluation on the testing task sets: $T_{\text{test,in}}$, $T_{\text{test,out}}^{(1)}$ and $T_{\text{test,out}}^{(2)}$.
- **Original.** It uses the sub-modules’ default configurations (see Table 3) for optimizing the target optimization problems in the optimization tasks. We note that Original baseline operates the AC tasks differently with ConfigX. Our ConfigX provide dynamic and flexible AC for each optimization step along the horizon. Original, on the

other hand, follows the default configurations from the start to the end.

- **Random.** It randomly selects a configuration value for each sub-modules in an algorithm structure, in each optimization step. This baseline and the Original baseline aid in demonstrating the learning effectiveness of ConfigX.

Performance Metric. The scale of the objective values across tasks can vary, to ensure the fairness of the comparison of baselines across tasks, we conduct a normalization process to restrict the objective value scales of different tasks in the same level. Considering minimization problem, we first calculate the maximum and minimum objective values in each task across all baselines and all runs:

$$\begin{aligned} Obj_{\max}^i &= \max_{b \in B, g \in [1, 51]} \{f_{b,g,0}^{i,*}\} \\ Obj_{\min}^i &= \min_{b \in B, g \in [1, 51]} \{f_{b,g,H}^{i,*}\} \end{aligned} \quad (20)$$

where $f_{b,g,0}^{i,*}$ and $f_{b,g,H}^{i,*}$ are the best objective values found in the g -th run of baseline b at optimization step 0 (initial step) and H (last step) on i -th task, H denotes the length of optimization horizon and B is the set of baselines including ConfigX, SMAC3, Original and Random. Obj_{\max}^i and Obj_{\min}^i denote the objective value upper and lower bounds of the i -th task. To make the performance metric consistent across all experiments in this paper, we calculate Obj_{\max} and Obj_{\min} for all tasks using the experiment data in Section 4.2 and fix them in the performance normalization in all experiments. Then we use these upper and lower bounds of each task to min-max normalize the performance of baseline b at optimization step t as:

$$Obj_{b,t} = \frac{1}{K \cdot N} \sum_{i=1}^{K \cdot N} \left[\frac{1}{51} \sum_{g=1}^{51} \frac{f_{b,g,t}^{i,*} - Obj_{\min}^i}{Obj_{\max}^i - Obj_{\min}^i} \right] \quad (21)$$

where $K \cdot N$ denotes the number of tasks. The corresponding min-max normalized performance used in our experimental results are computed as $(1 - Obj)$. This normalization process is applied on all performance results in the experiments.

E.3 Additional Experiment Results

Show Case on Advanced Algorithms One of the advantage in ConfigX against the other MetaBBO methods is that our ConfigX is capable of configuring any algorithm structures within the Modular-BBO’s algorithm space. We here demonstrate the practical usage of ConfigX by showcasing its adaptability for practical EAs such as SHADE (Tanabe and Fukunaga 2013) and MadDE (Biswas et al. 2021) which represent the first-rank optimization performance. We directly use the pre-trained ConfigX model to configure them and present the optimization performance of the pre-trained model and other baselines in Figure 6. The results show that: (a) Our pre-trained model is sufficient to boost performance of up-to-date EAs. (b) SMAC3 falls short in boosting such EAs since on the one hand, these EAs have intricate configuration spaces hence challenging the searching ability of SMAC3, and on the other hand SMAC3 searches for a good configuration for the whole optimization process hence not as flexible as ConfigX.

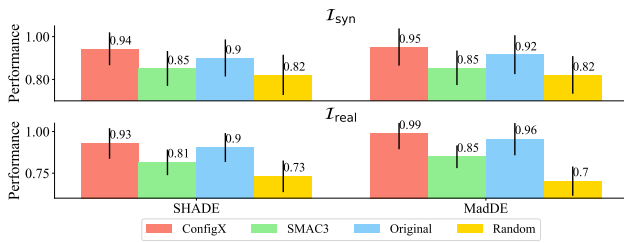


Figure 6: The performance on advanced DE tasks.

| | T_{train} | $T_{test,in}$ | $T_{test,out}^{(1)}$ | $T_{test,out}^{(2)}$ |
|----------|--------------|---------------|----------------------|----------------------|
| ConfigX | 527s / 7.03s | - / 7.14s | - / 8.64s | - / 7.11s |
| SMAC3 | 281s / 5.86s | 286s / 5.93s | - / 7.53s | 284s / 5.89s |
| Original | - / 5.73s | - / 5.76s | - / 7.49s | - / 5.72s |
| Random | - / 5.79s | - / 5.80s | - / 7.55s | - / 5.79s |

Table 4: The training / testing time efficiency of ConfigX and the baselines on the four task sets.

Time Efficiency Comparison In this section we investigate the time efficiency of ConfigX and the baselines. For training, we evaluate ConfigX by averaging its training time in 50 epochs and measure SMAC3’s per task training time with its default settings (i.e., 100 n_trails). For testing, we evaluate the averaged per task per run testing time. In Table 4 we present the averaged training / testing time on all four task sets, ‘-’ means no training time required. (a) Although ConfigX requires almost double training time of SMAC3 on T_{train} , ConfigX can zero-shot to unseen algorithm structures without further training time. SMAC3 requires scratch training for all algorithms and leads to a larger overall training time on all four task sets, which highlights the time efficiency advantage of ConfigX against SMAC3. (b) On the testing time, ConfigX takes more time than the three baselines, due to the network processing. But the superior performance of ConfigX proves the value of the extra runtime.

Train-Test Split Analysis In this section we conduct the experiments on different train-test splits to analyze the impact of different training and test set allocations. Concretely, we train ConfigX models on doubled and halved training tasks set with 64 and 16 DE algorithms generated from \mathcal{A}_{DE} respectively, combining with the 8 instances in \mathcal{I}_{syn} . Then we compare them with the model trained on normal size training task set with 32 DE algorithms on the three testing task sets $T_{test,in}$, $T_{test,out}^{(1)}$ and $T_{test,out}^{(2)}$. The results presented in Table 5 shows that increasing training instances slightly improves generalization, while reducing instances leads to performance degradation. However, considering the doubled training time and reduced training efficiency, the brought performance improvement is limited. Therefore in this paper we use 32 DE algorithms for training which balances the performance and training efficiency.

Sub-module Set Size Analysis To investigate how might the size of sub-module set impact the model’s performance, we construct a reduced sub-module set which only contains necessary sub-modules for complete DE

| | $T_{test,in}$ | $T_{test,out}^{(1)}$ | $T_{test,out}^{(2)}$ |
|----------------|--------------------------------------|--------------------------------------|--------------------------------------|
| ConfigX | 9.81E-01 ±7.33E-03 | 9.86E-01 ±2.64E-03 | 9.22E-01 ± 6.94E-03 |
| ConfigX-Double | 9.83E-01 ± 6.94E-03 | 9.87E-01 ± 2.86E-03 | 9.22E-01 ± 5.28E-03 |
| ConfigX-Half | 9.76E-01 ±8.63E-03 | 9.82E-01 ±9.11E-03 | 9.19E-01 ±9.01E-03 |

Table 5: Performance of ConfigX models trained with different training sets.

| | T'_{train} | $T_{test,in}$ | $T_{test,out}^{(1)}$ | $T_{test,out}^{(2)}$ |
|----------------|--------------------------------------|--------------------------------------|--------------------------------------|--------------------------------------|
| ConfigX | 9.84E-01 ±6.54E-03 | 9.81E-01 ± 7.33E-03 | 9.86E-01 ± 2.64E-03 | 9.22E-01 ± 6.94E-03 |
| ConfigX-Reduce | 9.87E-01 ± 6.88E-03 | 9.79E-01 ±7.55E-03 | 9.81E-01 ±7.69E-03 | 9.18E-01 ±8.31E-03 |

Table 6: Performance of ConfigX models trained with different sub-module sets.

algorithms: INITIALIZATION, MUTATION, CROSSOVER, BOUNDARY_CONTROL and SELECTION. Then we generate 32 DE algorithms from the reduced sub-module set and obtain a training task set T'_{train} with the 8 instances in \mathcal{I}_{syn} . The performance of ConfigX and the model trained on T'_{train} (denoted as ‘‘ConfigX-Reduce’’) is shown in Table 6. The results show that the narrowed sub-module set does not influence the RL learning effectiveness, while the generalization of the learned model is influenced. The model trained with limited sub-modules fails to apply its configuration experience on unseen sub-modules, which is consistent with our conclusions in Section 4.2.

References

- Aleti, A.; and Moser, I. 2016. A systematic literature review of adaptive parameter control methods for evolutionary algorithms. *ACM Computing Surveys (CSUR)*.
- Amoshahy, M. J.; Shamsi, M.; and Sedaaghi, M. H. 2016. A novel flexible inertia weight particle swarm optimization algorithm. *PLoS one*, 11(8): e0161558.
- Ans3t3gui, C.; Sellmann, M.; and Tierney, K. 2009. A gender-based genetic algorithm for the automatic configuration of algorithms. In *International Conference on Principles and Practice of Constraint Programming*.
- Arango, S. P.; Jomaa, H. S.; Wistuba, M.; and Grabocka, J. 2021. HPO-B: A Large-Scale Reproducible Benchmark for Black-Box HPO based on OpenML. In *Proceedings of the 35th Conference on Neural Information Processing Systems*.
- Arruda, L. V.; Swiech, M.; Delgado, M.; and Neves-Jr, F. 2008. PID control of MIMO process based on rank niching genetic algorithm. *Applied Intelligence*, 29(3): 290–305.
- Ba, J. L.; Kiros, J. R.; and Hinton, G. E. 2016. Layer normalization. In *Proceedings of the 30th Conference on Neural Information Processing Systems*.
- Baker, J. E. 2014. Adaptive selection methods for genetic algorithms. In *Proceedings of the first international confer-*

- ence on genetic algorithms and their applications, 101–106. Psychology Press.
- Biswas, S.; Saha, D.; De, S.; Cobb, A. D.; Das, S.; and Jalian, B. A. 2021. Improving differential evolution through Bayesian hyperparameter optimization. In *2021 IEEE Congress on Evolutionary Computation (CEC)*, 832–840.
- Brest, J.; Maučec, M. S.; and Bošković, B. 2021. Self-adaptive differential evolution algorithm with population size reduction for single objective bound-constrained optimization: Algorithm j21. In *2021 IEEE Congress on Evolutionary Computation (CEC)*, 817–824. IEEE.
- Cao, Y.; and Shen, Y. 2020. Bayesian active learning for optimization and uncertainty quantification in protein docking. *Journal of Chemical Theory and Computation*, 16(8): 5334–5347.
- Chen, A.; Dohan, D.; and So, D. 2024. EvoPrompting: language models for code-level neural architecture search. *Advances in Neural Information Processing Systems*, 36.
- Chen, J.; Ma, Z.; Guo, H.; Ma, Y.; Zhang, J.; and Gong, Y.-j. 2024. Symbol: Generating Flexible Black-Box Optimizers through Symbolic Equation Learning. In *The Twelfth International Conference on Learning Representations*.
- Das, S.; Mullick, S. S.; and Suganthan, P. N. 2016. Recent advances in differential evolution—an updated survey. *Swarm and Evolutionary Computation*, 27: 1–30.
- Deb, K.; Agrawal, R. B.; et al. 1995. Simulated binary crossover for continuous search space. *Complex systems*, 9(2): 115–148.
- Dobnikar, A.; Steele, N. C.; Pearson, D. W.; Albrecht, R. F.; Deb, K.; and Agrawal, S. 1999. A niched-penalty approach for constraint handling in genetic algorithms. In *Artificial Neural Nets and Genetic Algorithms: Proceedings of the International Conference in Portorož, Slovenia, 1999*, 235–243. Springer.
- Eimer, T.; Biedenkapp, A.; Reimer, M.; Adriaensen, S.; Hutter, F.; and Lindauer, M. 2021. DACBench: A benchmark library for dynamic algorithm configuration. *arXiv preprint arXiv:2105.08541*.
- Fialho, Á. 2010. *Adaptive operator selection for optimization*. Ph.D. thesis, Université Paris Sud-Paris XI.
- Finn, C.; Abbeel, P.; and Levine, S. 2017. Model-agnostic meta-learning for fast adaptation of deep networks. In *International Conference on Machine Learning*.
- Gehring, J.; Auli, M.; Grangier, D.; Yarats, D.; and Dauphin, Y. N. 2017. Convolutional sequence to sequence learning. In *International Conference on Machine Learning*, 1243–1252. PMLR.
- Goldberg, D. E.; and Deb, K. 1991. A comparative analysis of selection schemes used in genetic algorithms. In *Foundations of genetic algorithms*, volume 1, 69–93. Elsevier.
- Gong, W.; Fialho, A.; Cai, Z.; and Li, H. 2011. Adaptive strategy selection in differential evolution for numerical optimization: an empirical study. *Information Sciences*, 181(24): 5364–5386.
- Guo, H.; Ma, Y.; Ma, Z.; Chen, J.; Zhang, X.; Cao, Z.; Zhang, J.; and Gong, Y.-J. 2024. Deep Reinforcement Learning for Dynamic Algorithm Selection: A Proof-of-Principle Study on Differential Evolution. *IEEE Transactions on Systems, Man, and Cybernetics: Systems*.
- Gupta, A.; Fan, L.; Ganguli, S.; and Fei-Fei, L. 2022. Metamorph: learning universal controllers with transformers. In *International Conference on Learning Representations*. ICLR.
- Halton, J. H. 1960. On the efficiency of certain quasi-random sequences of points in evaluating multi-dimensional integrals. *Numerische Mathematik*, 2: 84–90.
- Hansen, N.; Auger, A.; Finck, S.; and Ros, R. 2010. *Real-parameter black-box optimization benchmarking 2010: Experimental setup*. Ph.D. thesis, INRIA.
- Holland, J. H. 1992. *Adaptation in natural and artificial systems: an introductory analysis with applications to biology, control, and artificial intelligence*. MIT press.
- Huang, C.; Li, Y.; and Yao, X. 2019. A survey of automatic parameter tuning methods for metaheuristics. *IEEE Transactions on Evolutionary Computation*.
- Hwang, H.; Vreven, T.; Janin, J.; and Weng, Z. 2010. Protein–protein docking benchmark version 4.0. *Proteins: Structure, Function, and Bioinformatics*.
- Islam, S. M.; Das, S.; Ghosh, S.; Roy, S.; and Suganthan, P. N. 2011. An adaptive differential evolution algorithm with novel mutation and crossover strategies for global numerical optimization. *IEEE Transactions on Systems, Man, and Cybernetics, Part B (Cybernetics)*, 42(2): 482–500.
- Jansen, T. 2002. On the analysis of dynamic restart strategies for evolutionary algorithms. In *Parallel Problem Solving from Nature—PPSN VII: 7th International Conference Granada, Spain, September, 2002 Proceedings 7*, 33–43.
- Joe, S.; and Kuo, F. Y. 2008. Constructing Sobol sequences with better two-dimensional projections. *SIAM Journal on Scientific Computing*, 30(5): 2635–2654.
- Kadavy, T.; Viktorin, A.; Kazikova, A.; Pluhacek, M.; and Senkerik, R. 2023. Impact of boundary control methods on bound-constrained optimization benchmarking. In *Proceedings of the Companion Conference on Genetic and Evolutionary Computation*, 25–26.
- Kazimpour, B.; Li, X.; and Qin, A. K. 2014. A review of population initialization techniques for evolutionary algorithms. In *2014 IEEE Congress on Evolutionary Computation (CEC)*, 2585–2592. IEEE.
- Kennedy, J.; and Eberhart, R. 1995. Particle swarm optimization. In *Proceedings of ICNN’95-International Conference on Neural Networks*, volume 4, 1942–1948. IEEE.
- Li, X.; Engelbrecht, A.; and Epitropakis, M. G. 2013. Benchmark functions for CEC’2013 special session and competition on niching methods for multimodal function optimization. *RMIT University, Evolutionary Computation and Machine Learning Group, Australia, Tech. Rep*.
- Li, X.; Tang, K.; Omidvar, M. N.; Yang, Z.; Qin, K.; and China, H. 2013. Benchmark functions for the CEC 2013 special session and competition on large-scale global optimization. *Gene*, 7(33): 8.

- Li, X.; Wu, K.; Li, Y. B.; Zhang, X.; Wang, H.; and Liu, J. 2024. GLHF: General Learned Evolutionary Algorithm Via Hyper Functions. *arXiv preprint arXiv:2405.03728*.
- Lian, H.; Ma, Z.; Guo, H.; Huang, T.; and Gong, Y.-J. 2024. RLEMMO: Evolutionary Multimodal Optimization Assisted By Deep Reinforcement Learning. In *Proceedings of the Genetic and Evolutionary Computation Conference*, 683–693.
- Liang, J. J.; Qin, A. K.; Suganthan, P. N.; and Baskar, S. 2006. Comprehensive learning particle swarm optimizer for global optimization of multimodal functions. *IEEE transactions on evolutionary computation*, 10(3): 281–295.
- Liang, J.-J.; and Suganthan, P. N. 2005. Dynamic multi-swarm particle swarm optimizer. In *Proceedings 2005 IEEE Swarm Intelligence Symposium, 2005. SIS 2005.*, 124–129. IEEE.
- Lindauer, M.; Eggensperger, K.; Feurer, M.; Biedenkapp, A.; Deng, D.; Benjamins, C.; Ruhkopf, T.; Sass, R.; and Hutter, F. 2022. SMAC3: A Versatile Bayesian Optimization Package for Hyperparameter Optimization. *Journal of Machine Learning Research*, 23(54): 1–9.
- Liu, Q.; Du, S.; Van Wyk, B. J.; and Sun, Y. 2020. Niching particle swarm optimization based on Euclidean distance and hierarchical clustering for multimodal optimization. *Nonlinear Dynamics*, 99: 2459–2477.
- Lunacek, M.; and Whitley, D. 2006. The dispersion metric and the CMA evolution strategy. In *Proceedings of the 8th Annual Conference on Genetic and Evolutionary Computation*, 477–484.
- Lynn, N.; and Suganthan, P. N. 2017. Ensemble particle swarm optimizer. *Applied Soft Computing*, 55: 533–548.
- Ma, H.; Shen, S.; Yu, M.; Yang, Z.; Fei, M.; and Zhou, H. 2019. Multi-population techniques in nature inspired optimization algorithms: A comprehensive survey. *Swarm and Evolutionary Computation*, 44: 365–387.
- Ma, Z.; Chen, J.; Guo, H.; Ma, Y.; and Gong, Y.-J. 2024a. Auto-configuring Exploration-Exploitation Tradeoff in Evolutionary Computation via Deep Reinforcement Learning. In *Proceedings of the Genetic and Evolutionary Computation Conference*, 1497–1505.
- Ma, Z.; Guo, H.; Chen, J.; Li, Z.; Peng, G.; Gong, Y.-J.; Ma, Y.; and Cao, Z. 2023. MetaBox: A Benchmark Platform for Meta-Black-Box Optimization with Reinforcement Learning. In *Advances in Neural Information Processing Systems*, volume 36.
- Ma, Z.; Guo, H.; Gong, Y.-J.; Zhang, J.; and Tan, K. C. 2024b. Toward Automated Algorithm Design: A Survey and Practical Guide to Meta-Black-Box-Optimization. *arXiv preprint arXiv:2411.00625*.
- MacKerell Jr, A. D.; Bashford, D.; Bellott, M.; Dunbrack Jr, R. L.; Evanseck, J. D.; Field, M. J.; Fischer, S.; Gao, J.; Guo, H.; Ha, S.; et al. 1998. All-atom empirical potential for molecular modeling and dynamics studies of proteins. *The Journal of Physical Chemistry*, 102(18): 3586–3616.
- Mahdavi, S.; Rahnamayan, S.; and Deb, K. 2016. Center-based initialization of cooperative co-evolutionary algorithm for large-scale optimization. In *2016 IEEE Congress on Evolutionary Computation (CEC)*, 3557–3565. IEEE.
- Mallipeddi, R.; Suganthan, P. N.; Pan, Q.-K.; and Tasgetiren, M. F. 2011. Differential evolution algorithm with ensemble of parameters and mutation strategies. *Applied Soft Computing*, 11(2): 1679–1696.
- McKay, M. D.; Beckman, R. J.; and Conover, W. J. 2000. A comparison of three methods for selecting values of input variables in the analysis of output from a computer code. *Technometrics*, 42(1): 55–61.
- Michalewicz, Z. 2013. *Genetic algorithms+ data structures= evolution programs*. Springer Science & Business Media.
- Peng, F.; Tang, K.; Chen, G.; and Yao, X. 2009. Multi-start JADE with knowledge transfer for numerical optimization. In *2009 IEEE Congress on Evolutionary Computation*, 1889–1895. IEEE.
- Peng, H.; Han, Y.; Deng, C.; Wang, J.; and Wu, Z. 2021. Multi-strategy co-evolutionary differential evolution for mixed-variable optimization. *Knowledge-Based Systems*, 229: 107366.
- Peram, T.; Veeramachaneni, K.; and Mohan, C. K. 2003. Fitness-distance-ratio based particle swarm optimization. In *Proceedings of the 2003 IEEE Swarm Intelligence Symposium. SIS'03 (Cat. No. 03EX706)*, 174–181. IEEE.
- Pierce, B. G.; Wiehe, K.; Hwang, H.; Kim, B.-H.; Vreven, T.; and Weng, Z. 2014. ZDOCK server: interactive docking prediction of protein–protein complexes and symmetric multimers. *Bioinformatics*, 30(12): 1771–1773.
- Poláková, R.; Tvrdík, J.; and Bujok, P. 2014. Controlled restart in differential evolution applied to CEC2014 benchmark functions. In *2014 IEEE Congress on Evolutionary Computation (CEC)*, 2230–2236. IEEE.
- Pool, J. E.; and Nielsen, R. 2007. Population size changes reshape genomic patterns of diversity. *Evolution*, 61(12): 3001–3006.
- Qin, A. K.; and Suganthan, P. N. 2005. Self-adaptive differential evolution algorithm for numerical optimization. In *2005 IEEE Congress on Evolutionary Computation*, volume 2, 1785–1791. IEEE.
- Schulman, J.; Wolski, F.; Dhariwal, P.; Radford, A.; and Klimov, O. 2017. Proximal policy optimization algorithms. *arXiv preprint arXiv:1707.06347*.
- Shahriari, B.; Swersky, K.; Wang, Z.; Adams, R. P.; and De Freitas, N. 2015. Taking the human out of the loop: A review of Bayesian optimization. *Proceedings of the IEEE*, 104(1): 148–175.
- Shami, T. M.; El-Saleh, A. A.; Alswaitti, M.; Al-Tashi, Q.; Summakieh, M. A.; and Mirjalili, S. 2022. Particle swarm optimization: A comprehensive survey. *IEEE Access*, 10: 10031–10061.
- Sharma, M.; Komninos, A.; López-Ibáñez, M.; and Zakakov, D. 2019. Deep reinforcement learning based parameter control in differential evolution. In *Proceedings of the Genetic and Evolutionary Computation Conference*, 709–717.

- Shukla, A.; Pandey, H. M.; and Mehrotra, D. 2015. Comparative review of selection techniques in genetic algorithm. In *2015 International Conference on Futuristic Trends on Computational Analysis and Knowledge Management (ABLAZE)*, 515–519. IEEE.
- Sobol, I. 1967. The distribution of points in a cube and the accurate evaluation of integrals (in Russian) *Zh. Vychisl. Mat. i Mater. Phys.*, 7: 784–802.
- Song, L.; Gao, C.; Xue, K.; Wu, C.; Li, D.; Hao, J.; Zhang, Z.; and Qian, C. 2024. Reinforced In-Context Black-Box Optimization. *arXiv preprint arXiv:2402.17423*.
- Spears, W. M. 1995. Adapting Crossover in Evolutionary Algorithms. In *Evolutionary Programming IV: Proceedings of the Fourth Annual Conference on Evolutionary Programming*, 367.
- Stanovov, V.; Akhmedova, S.; and Semenkin, E. 2021. NL-SHADE-RSP algorithm with adaptive archive and selective pressure for CEC 2021 numerical optimization. In *2021 IEEE Congress on Evolutionary Computation (CEC)*, 809–816. IEEE.
- Storn, R.; and Price, K. 1997. Differential evolution—a simple and efficient heuristic for global optimization over continuous spaces. *Journal of Global Optimization*, 11: 341–359.
- Sun, J.; Liu, X.; Bäck, T.; and Xu, Z. 2021. Learning adaptive differential evolution algorithm from optimization experiences by policy gradient. *IEEE Transactions on Evolutionary Computation*, 25(4): 666–680.
- Tan, Z.; and Li, K. 2021. Differential evolution with mixed mutation strategy based on deep reinforcement learning. *Applied Soft Computing*, 111: 107678.
- Tan, Z.; Tang, Y.; Li, K.; Huang, H.; and Luo, S. 2022. Differential evolution with hybrid parameters and mutation strategies based on reinforcement learning. *Swarm and Evolutionary Computation*.
- Tanabe, R.; and Fukunaga, A. 2013. Success-history based parameter adaptation for differential evolution. In *2013 IEEE Congress on Evolutionary Computation*, 71–78. IEEE.
- Tanabe, R.; and Fukunaga, A. S. 2014. Improving the search performance of SHADE using linear population size reduction. In *2014 IEEE Congress on Evolutionary Computation (CEC)*, 1658–1665. IEEE.
- Tao, X.; Li, X.; Chen, W.; Liang, T.; Li, Y.; Guo, J.; and Qi, L. 2021. Self-Adaptive two roles hybrid learning strategies-based particle swarm optimization. *Information Sciences*, 578: 457–481.
- Tomassini, M.; Vanneschi, L.; Collard, P.; and Clergue, M. 2005. A study of fitness distance correlation as a difficulty measure in genetic programming. *Evolutionary Computation*, 13(2): 213–239.
- Toulouse, M.; Crainic, T. G.; and Gendreau, M. 1996. *Communication issues in designing cooperative multi-thread parallel searches*. Springer.
- Vanschoren, J.; Van Rijn, J. N.; Bischl, B.; and Torgo, L. 2014. OpenML: networked science in machine learning. *ACM SIGKDD Explorations Newsletter*, 15(2): 49–60.
- Vaswani, A.; Shazeer, N.; Parmar, N.; Uszkoreit, J.; Jones, L.; Gomez, A. N.; Kaiser, Ł.; and Polosukhin, I. 2017. Attention is all you need. *Advances in Neural Information Processing Systems*.
- Wang, Y.; Cai, Z.; and Zhang, Q. 2011. Differential evolution with composite trial vector generation strategies and control parameters. *IEEE Transactions on Evolutionary Computation*, 15(1): 55–66.
- Williams, R. J. 1992. Simple statistical gradient-following algorithms for connectionist reinforcement learning. *Machine Learning*.
- Wu, D.; and Wang, G. G. 2022. Employing reinforcement learning to enhance particle swarm optimization methods. *Engineering Optimization*, 54(2): 329–348.
- Xue, K.; Xu, J.; Yuan, L.; Li, M.; Qian, C.; Zhang, Z.; and Yu, Y. 2022. Multi-agent dynamic algorithm configuration. *Advances in Neural Information Processing Systems*, 35: 20147–20161.
- Yang, X.; Wang, R.; and Li, K. 2024. Meta-Black-Box Optimization for Evolutionary Algorithms: Review and Perspective. *Available at SSRN 4956956*.
- Ye, C.; Li, C.; Li, Y.; Sun, Y.; Yang, W.; Bai, M.; Zhu, X.; Hu, J.; Chi, T.; Zhu, H.; et al. 2023. Differential evolution with alternation between steady monopoly and transient competition of mutation strategies. *Swarm and Evolutionary Computation*, 83: 101403.
- Zhabitskaya, E.; and Zhabitsky, M. 2013. Asynchronous differential evolution with restart. In *Numerical Analysis and Its Applications: 5th International Conference, NAA 2012, Lozenetz, Bulgaria, June 15-20, 2012, Revised Selected Papers 5*, 555–561. Springer.
- Zhang, J.; and Sanderson, A. C. 2009. JADE: adaptive differential evolution with optional external archive. *IEEE Transactions on Evolutionary Computation*, 13(5): 945–958.